A STUDY OF THE CHARACTERISTICS OF CONVERGING VORTEX FLOW

by

Lieut. E.P. Levitt, USN

May, 1949

Thesis
L6

Library
U. S. Naval Postgraduate School
Annapolis, Md.

A STUDY OF THE CHARACTERISTICS OF CONVERGING VORTEX FLOW

by

Lieutenant Ben B. Levitt, United States Navy

Submitted to the Faculty of
Rensselaer Polytechnic Institute
in partial fulfillment of
the requirements for the degree of
Master of Science.

Troy, New York
June, 1949

SUMMARY

The purpose of this investigation was to study the characteristics of a converging vortex in a real gas, and to determine if it was possible to reach superacoustic flow in a vortex.

Air at a high angular velocity was introduced at the periphery of a vortex tube. The air then flowed into an annular passage and converged into a constant area tube. Tests were run both with and without a convergence cone in the converging section of the vortex tube.

It was found that superacoustic flow could be obtained, and that greater velocities were produced with the convergence cone present. A large loss in angular momentum occurred during the convergence, this loss being greater with the convergence cone removed. It was also shown that the convergence of a vortex in an annular area tends to bring the flow very rapidly into a condition of equilibrium. In this condition, no viscous forces are acting and there is no heat transfer between adjacent layers of air.

SYMBOLS

A = Annular area

g = Acceleration of gravity

M = Mach number

MV = Millivolt reading of potentiometer

m = Mass

P = Static pressure

P_o = Total pressure

P_{op_1} = Pressure ahead of metering nozzle

P_{op_2} = Pressure in pelnum chamber

ΔP = Pressure drop across metering nozzle

R = Gas constant (53.3)

r = Radius

T = Static temperature

T_o = Total temperature

T_{o_p} = Total temoerature in pelnum chamber

v = Velocity

w = Weight flow

γ = Adiabatic gas constant (1.395)

λ = Angular momentum

η = Convergence efficiency

ω = Angular velocity

ρ = Specific density

SUBSCRIPTS:

c = conditions at vortex center

w = conditions at vortex wall

V, A, B, C, 1, 2, 3------12, refer to vortex tube stations

TABLE OF CONTENTS

	Page
Summary	
Symbols	
Introduction	1
Equipment and Procedure	4
Theory	18
Results and Discussion	25
Conclusions	35
Recommendations	36
Bibliography	
Sample Calculations	
Table and Curves	
Photographs	

INTRODUCTION

Classical aerodynamicists refer to a vortex as a mathematical concept obtainable only in an ideal fluid. This concept requires that the velocity become infinite and the pressure zero at the vortex center, an impossibility in any real fluid. Therefore the use of the term "vortex" has been extended from the strictly classical definition to include any form of continuously rotative fluid motion.

A French scientist, G. J. Ranque, published a paper in 1933 describing the low temperatures he had obtained in the center of air set into a vortex motion. During World War II, Rudolph Hilsch, a German, extended Ranque's experiments and separated the hot air from the cold air in a vortex tube. This so-called Hilsch tube became popularized as a "molecule separator" since it was believed that it blew the hot air molecules out of one end of the tube and the cold molecules out of the other end.

In 1946 Hilsch's work became known in this country, and shortly thereafter the General Electric Research Laboratory made an analysis of the device for use in refrigeration.[2] They concluded that the efficiency for refrigeration was very low and the operating cost high.

Professor Neil P. Bailey, head of the Department of Mechanical Engineering, Rensselaer Polytechnic Institute,

Troy, N. Y. and members of his staff, proposed a theory that a vortex in an actual gas approaches a condition of equilibrium such that the fluid mass rotates as a solid body. Since there is no relative motion between adjacent fluid layers in this condition, there would be no heat transfer and no viscous forces acting. In order to check this theory experimentally, W. C. Vickrey[3] induced a vortex in a two-inch tube. His results indicated that an equilibrium plane did exist in the vortex tube and conformed fairly well to the theory, although he worked only at low weight flows. Several months later, L. M. Zubko[4] repeated Vickrey's experiment at higher weight flows and using a four-inch vortex tube. Zubko also found an equilibrium plane, and in addition he indicated the presence of a thin longitudinal shell which rotated at a constant angular velocity equal to the angular velocity of the equilibrium plane.

The object of this investigation is to carry on a bit further into the study of vortex characteristics in an actual gas. Both Vickrey and Zubko used vortex tubes of constant cross-sectional area. The theory, however, allows for a convergence (or divergence) of the vortex. A converging vortex is present in the tail cone of a jet engine when the turbine is not operating at design speed. A study of this problem might therefore be of some practical

value. In addition, a point of great interest is the fact the the theory indicates that superacoustic flow is possible in a convering vortex.

It was, then, the purpose of this report to investigate the characteristics of a converging vortex in an actual gas, and to determine if superacoustic flow is possible. The investigation was conducted in the Mechanical Engineering Department, Rensselaer Polytechnic Institute, Troy, N.Y., during the period February-May, 1949.

The author wishes to express his gratitude to Professor Neil P. Bailey and Mr. Andrew J. Shine for their guidance and advice, and to members of the Machine Shop staff for their patience and skill.

EQUIPMENT AND PROCEDURE

A schematic diagram of the test set-up is shown in Figure 1. The electric motor, driving the compressor, was a Westinghouse three-phase, 60 cycle, 220-400 volts, 50 horsepower motor with a rated full load speed of 1175 rpm. It was connected directly to the air compressor, which was a six cylinder Schram, Model 210, rated at 206 cubic feet per minute of standard air at 1175 rpm. From the compressor the air was led through a water aftercooler and oil separator, and thence into the receiver tank. The motor automatically cut out the compressor when the receiver tank pressure reached 100 psi gage, and cut it back in when the pressure reached 80 psi gage. To assure a continuous source of supply air, a bleed valve was provided downstream of the receiver tank. By regulating the bleed valve, the air compressor would stay on the line during the entire run.

The air was led into the plenum chamber through a course and a fine flow control valve. A 3/4-inch metering nozzle was placed in the plenum chamber. The pressure was measured forward of the metering nozzle on a mercury manometer or pressure gage (P_{op_1}). The pressure drop across the nozzle could be measured either on a differential mer-

cury or water manometer (ΔP). The total temperature was measured downstream of the metering nozzle (T_{op}). Knowing the area of the nozzle, P_{op_1}, ΔP, and T_{op} it was possible to calculate the weight flow. An additional pressure tap was placed downstream of the metering nozzle (P_{op_2}) in order to obtain a total pressure entering the vortex valve, free from any diffusion or metering nozzle losses.

A diagram of the vortex tube used in this investigation is shown in Figure 2. The converging section was turned from a laminated block of well-seasoned maple, and had a wall thickness varying from 3/4-inch at maximum diameter to 1/2-inch at the constant diameter section. The inside taper was linear except for slight fillets at both ends to facilitate the air flow, and the inside surface was well polished. A copper tube of 1 1/4-inch nominal inside diameter was sweated into the neck of the converging section. It was secured in place by a thin plate soldered to the outside of the tubing, and screwed into the maple neck. The brass tubing was 13 inches long, with a wall thickness of 1/16-inch, and was polished to an inside diameter of 1.269 inches.

The vortex valve was originally designed by Professor Neil P. Bailey for other experimental purposes, and was the same valve as used by Vickrey and Zubko. Briefly, it consisted of twenty-four adjustable angle vanes secured to the

periphery of a 3/16-inch brass disc of two and three-quarter inch diameter. The air flows radially outward along the disc, is turned in the vanes, and enters the vortex tube with a high angular velocity. In all the tests made in this investigation the vanes were set at an angle of ten degrees to the peripheral tangent, in order to reduce the radial component of flow as much as possible. Figure 3 is a diagram of the vortex valve, and Reference (1) is a detailed report on its performance.

The vortex cone was turned from a solid block of well-seasoned maple, and was highly polished to reduce frictional effects. The cone was secured to the vortex valve disc by three screws countersunk into the face of the disc. The taper of the cone was such that the annular area between cone and wall remained constant and equal to the area of the brass tubing. In designing the cone, allowance was made for taper of the wall at the extremes so that the annular area would remain truly constant. The length of the cone was 2.40 inches from its tip to the back face of the vortex valve disc. This provided the cone with a diameter-to-length ratio of 1.147. This ratio should be as great as possible to minimize frictional losses as the vortex converges. However, it was felt that if the ratio were made much larger, separa-

tion might occur at the cone surface. In future investigations it would be of interest to determine the effect of the vortex cone proportions. A table of coordinates of the vortex cone is given in Figure 2.

A wall pressure tap was provided between the plenum chamber and the vortex valve. In testing, however, it was found that this pressure was essentially the same as that measured downstream from the metering nozzle (P_{op_2}), the difference not being detectable on a mercury manometer up to 60 inches gage pressure. This pressure tap was therefore tied off, and the value of P_{op_2} used as the true total pressure entering the vortex valve. A second wall pressure tap was placed in the plate to which the vortex tube was secured (P_v). It was located at a radius just equal to that of the vortex valve disc periphery, and approximately mid-way between the vanes and the wall. The purpose of this tap was to provide a means of computing the velocity leaving the vanes and entering the vortex tube.

Three instrumentation holes were provided down the converging section of the vortex tube at distances of 0.580, 1.425, and 2.275 inches normally from the inside face of the plate to which the vortex tube was secured. These holes were 9/16-inch except for the last 1/4-inch which was drilled and tapped to accommodate the 1/4-inch root of the radial

probes. Twelve instrumentation holes of the same size were provided in the constant area section of the vortex tube. The first hole was placed so that its center was one-tenth inch from the tip of the vortex cone, and the remaining holes were placed with their centers exactly one inch apart. It was necessary to solder a brass strip along the length of the vortex tube in order to increase its wall thickness to the 1/4-inch required by the radial probes. In this report the instrumentation holes are referred to as stations, and are labeled A, B, and C down the converging section and thence consecutively from 1 to 12 down the constant area section of the vortex tube.

When the vortex tube is in operation, a low pressure exists at the center and a high pressure at the periphery. Since the vortex is discharging into atmospheric air of constant pressure, an unstable condition exists at the discharge end of the tube. The low pressure at the center creates what Vickrey has termed a "back-flow" into the tube. This back-flow momentarily compensates the low pressure, but the vortex quickly rebuilds the low pressure area and the back-flow starts again. This cycle, of course, occurs with very high frequency, and the resulting noise is of such high pitch that it becomes unbearable at higher weight flows. In an attempt to overcome this difficulty and to

eliminate the back-flow, both Vickrey and Zubko used adjustable nose cones at the discharge end of the vortex tube. When the nose cone was positioned so that the noise was eliminated, it was assumed that all the back-flow into the vortex tube had been cut out. This author ran several preliminary tests on the adjustable nose cone and found that its exact position, even after the noise had been eliminated, had a considerable effect on the character of the flow. If the nose cone was positioned to just eliminate the noise, a small back-flow still existed down the sides of the cone. If the cone was moved in a little too far it created a back pressure on the flow and caused the vortex to "fill in" to some extent the low pressure at its center. Furthermore, the position of the nose cone was dependent on the weight flow, making it extremely difficult to position the cone properly to reproduce data. If a nose cone was not used the back-flow was so great that the value of the data obtained was highly questionable.

In an effort to overcome this problem, Professor Neil P. Bailey suggested that the vortex be permitted to enlarge suddenly into a "can" attached at the discharge end of the vortex tube. The flow would then discharge to the atmosphere at a constant pressure through holes placed about the periphery of the can. The author carried out

this suggestion and found it to work successfully. However, both the diameter of the can and the hole area was critical, it being necessary to determine both of these factors experimentally for each desired weight flow. Since this would prove extremely burdensome in extensive testing, a new method for eliminating the back-flow was sought.

After experimenting with several devices, the author found that a "self-adjusting" nose cone seemed to serve the purpose very well. This consisted simply of a nose cone which was allowed a single degree of axial freedom. The cone was machined from cast aluminum and fitted with a half-inch steel shaft two inches in length in its back face. The steel shaft rode in an aluminum sleeve of quarter-inch wall thickness, and when oiled made an easy sliding fit. The sleeve was rigidly secured to a stand on the testing table and positioned so that the nose cone would be exactly centered with the discharge end of the vortex tube. As the weight flow in the vortex tube was changed, the cone would slide inward or outward accordingly and adjust itself to the position required by the flow. All the noise was eliminated as well as the back-flow. No back-flow could be detected at any weight flow either by observing the position of threads attached to the surface of the cone, or by the direction in which the radial total pressure probe pointed

when inserted at stations near the discharge end of the vortex tube.

It was recognized that the nose cone angle would be critical, and that ideally the cone should be tapered to fit the pressure gradient existing across the vortex at the discharge. This fact was substantiated in later testing when the convergence cone was removed from the vortex tube (to be discussed further). An included nose cone angle of 80 degrees had been used on all previous tests, and had been found to work well at all weight flows. However, when the convergence cone was removed the flow was altered to such an extent that the 80 degree nose cone was practically worthless, it being necessary to hold it in position just as were the cones used by Vickrey and Zubko. After testing several nose cone sizes, it was found that a nose cone of 40 degrees included angle proved satisfactory for the new flow. This angle evidently conformed the closest to the discharge radial pressure distribution. Therefore, in all the testing done in this investigation a nose cone of 80 degree included angle was used, except in those runs in which the convergence cone was removed from the vortex tube a 40 degree nose cone was used.

Since it was desired to probe the vortex tube axially, it was necessary to drill a hole axially through the center

of the nose cone and shaft to accommodate the probe. This gave the additional advantage of providing a rigid 2 1/2-inch support for the probe at the vortex tube discharge. The hole was drilled with enough clearance to permit the probe to slide easily in the nose cone without binding. In this manner the axial probe could be slid inward or outward without disturbing the position of the nose cone relative to the vortex tube. It is possible that a small amount of leakage occurred between the probe and the cone, but if so it was very slight and probably negligible. When the axial probe was not in use, it was removed from the cone and the hole was closed off by covering the shaft end with tape.

Two axial probes were used, one for measuring the center pressure, and the other for measuring center temperature. Both probes were made of stiff hollow steel, .099 inches in diameter and 21 inches in length. The inside end of the pressure probe was filed off smoothly, while tothe outside end a rubber tube fitting was soldered. Pressures were read on a mercury manometer. Through the temperature probe a Leeds and Northrup iron-constantan thermocouple of No. 30 gage wire was fed. The hot junction bead was encased with a Duco Cement. The cement was sanded down to a smooth finish having the same diameter as the probe, and with just the tip of the bead exposed. It was thought this would

serve to reduce the effect of any heat transfer up or down the steel probe, although the temperature gradient along the vortex center was relatively small. Iron-constantan thermocouple wires were chosen since they give the highest millivolt-per-degree response. A cold junction of 32 degrees Fahrenheit was maintained in an ice bath. A Leeds and Northrup potentiometer was used in all temperature work. Since no flow existed in the center of the vortex where the axial probes were to be used, it was not necessary to calibrate them. The thermocouple was simply tested at 32 degrees Fahrenheit and 212 degrees Fahrenheit and was found to give accurate readings.

When the axial probes were inserted into the vortex more than about three inches, depending on the weight flow, it was found that considerable vibration was set up even after the probe had been aligned with the vortex center as accurately as possible. This was extremely undesirable not only because of accuracy of the readings obtained, but also because the vibration would bend the probe and cause the nose cone to bind on it. If the movement of the nose cone were restricted, of course, it could not perform its function of properly regulating the flow. To overcome this difficulty it was necessary to give additional support to the end of the axial probes. In order to accomplish this a "spider" was

secured to the probe two inches from its end. This consisted of a small brass collar to which was soldered three-euqally spaced legs of stiff steel wire. This additional support held the probe rigidly centered in the vortex tube without restricting its axial freedom, since the spider slid freely along the walls of the vortex tube when the probe was moved. This system proved very satisfactory at all weight flows, the vibration being completely eliminated. It was felt that the disturbance which the spider support would create in the vortex would not be serious since it was placed at a point two inches downstream from the end of the probe. Actually, due to the vortex motion of the flow, the distance that the air travels from the end of the probe to the spider support is much greater than two inches.

The outside end of the axial probes were rigidly secured to a crank and spindle device which was calibrated in inches to give the axial position of the probe in the vortex tube.

Two radial probes were also used in this investigation, one to measure total pressure and the other to measure total temperature. These probes were the same ones designed and used by Zubko in his work on vortex flow, and a complete description of them are available in Reference (4). No calibration corrections were used with the data obtained

with these probes since the total pressure corrections were extremely small and the total temperature readings had a maximum error of only 2.5 percent at Mach 0.9. Since only the temperature differences were of primary importance, it was felt that the calibration correction could be safely neglected.

To obtain the wall static pressure readings, a brass tap was made which could be screwed in at any station. When in position the tap was flush with the inside wall of the vortex tube, and from a No. 60 drill hole the pressure was let to a mercury manometer. When a station was not being used to obtain data, it was sealed off with a brass plug which made a flush fit with the inside wall of the vortex tube.

Tests were conducted at four different weight flows, and will be referred to hereafter as the gage pressure existing on the vortex valve (P_{op2}). These pressures were 40, 60, 80, and 100 inches of mercury gage. The 100-inch run was very close to the limit of air flow from the compressor. Originally it had been planned to test at only the first three flows, but when supersonic flow was not found it was decided to run an additional test at maximum compressor output.

The procedure followed in obtaining the data was to first probe axially for center pressure and temperature.

The axial probes were then removed and total and static wall pressure measured at each station, as well as the total temperature where desired. In this manner only one probe was present in the vortex tube at any time, and the resulting flow disturbance was kept at a minimum.

It should be noted here that the stations were not probed radially as was done by Vickrey and Zubko. It was believed that an equilibrium station could be found from the center pressure, wall pressure, and wall Mach number alone. The location of an equilibrium station was necessary in order to evaluate the angular momentum with the theoretical equations. The equilibrium station is the plane at which the air rotates with a solid body motion, no viscous forces or heat transfer being present between adjacent flow radii. All of the theoretical equations are built up on this type of flow.

Since no equilibrium station could be found in the 40 inch run, total pressure and temperature measurements were not taken down the converging section of the vortex tube for this run.

It was believed that the wall Mach numbers might be increased by removing the convergence cone from the vortex tube. Consequently, the 60, 80 and 100 inch runs were repeated with the convergence cone out. It was quickly seen,

however, that just the reverse was true, so that extensive data was not taken for these runs. No axial probing was done with the convergence cone removed.

In all tests it was necessary to wait about an hour for the compressor to settle down so that the supply air in the plenum chamber would reach a steady value, and the vortex tube would be uniformly heated.

Photographs of the equipment are included at the end of this report.

THEORY

Professor Neil P. Bailey's theory of a free vortex cone in a real gas is based on the assumptions that the vortex will approach a condition such that no viscous forces are acting and no heat transfer is present along the vortex radius. This requires that the flow rotate as a solid body. In order to facilitate further discussion, that part of the theory which applies to this investigation will be presented here.

The pressure present at any radius must be balanced by the centrifugal force due to rotation,

$$2\pi r\,(dp) = \frac{v^2}{r}\,(dm) \qquad (1)$$

But

$$(dm) = 2\pi r \rho\,(dr) \qquad (2)$$

So equation (1) becomes,

$$(dp) = \frac{v^2}{r}\,\rho\,(dr) \qquad (3)$$

For solid body rotation,

$$v = \omega r \qquad (4)$$

So equation (3) becomes,

$$(dp) = \omega^2 r \rho\,(dr) \qquad (5)$$

But

$$\rho = \frac{p}{g R T} \qquad (6)$$

So equation (5) reduces to,

$$\frac{(dp)}{P} = \frac{\omega^2 r}{g R T} \quad (dr) \qquad \text{(7)}$$

Since ω and T ,are constant for solid body rotation, equation (7) may now be integrated between center and wall conditions.

$$\int_{P_c}^{P_w} \frac{(dP)}{P} = \frac{\omega^2}{g R T} \int_{o}^{r_w} r \, (dr) \qquad \text{(8)}$$

or,

$$\log_e \frac{P_w}{P_c} = \frac{\omega^2 \ r_w^2}{2 \ g \ R \ T} \qquad \text{(9)}$$

However, since,

$$\frac{\omega^2 \ r_w^2}{\gamma g \ R \ T} = M_w^2 \qquad \text{(10)}$$

Equation (9) may be written as

$$\log_e \frac{P_w}{P_c} = \frac{\gamma M_w^2}{2} \qquad \text{(11)}$$

or,

$$\frac{P_w}{P_c} = e^{\frac{\gamma}{2} M_w^2} \qquad \text{(12)}$$

Now from equations (2) and (6), the total mass involved in a unit length of vortex is

$$(dm) = \frac{2 \pi r P}{g R T} \quad (dr) \qquad \text{(13)}$$

Equation (9) is valid for conditions at any radius so that it may be used to eliminate the pressure term from equation (13),

$$\int_0^{r_w} (dm) = \int_0^{r_w} \frac{2\pi r P_c}{g R T} e^{\frac{\omega^2 r^2}{2 g R T}} (dr) \qquad (14)$$

or,

$$m = \frac{2\pi P_c}{\omega^2} \left[e^{\frac{\omega^2 r_w^2}{2 g R T}} - 1 \right] \qquad (15)$$

which may be written as

$$m = \frac{2\pi P_c}{\omega^2} \left[e^{\frac{\gamma}{2} M_w^2} - 1 \right] \qquad (16)$$

Now the angular momentum, or moment of momentum, of a unit length of vortex annulus is,

$$(d\lambda) = vr\,(dm) \qquad (17)$$

Combining equations (2) and (6) to eliminate mass from (17), and substituting equation (4) for velocity,

$$(d\lambda) = \omega r^2\, 2\pi r \rho\,(dr) = \frac{2\pi\omega r^3 P}{g R T}\,(dr) \qquad (18)$$

Again extending equation (9) to eliminate the pressure term from (18),

$$(d\lambda) = \frac{2\pi\omega r^3 P_c}{gRT} e^{\frac{\omega^2 r^2}{2 g R T}} (dr) \qquad (19)$$

Equation (19) may now be integrated, since ω, P_c, and T are constants.

$$\int_0^{r_w} (d\lambda) = \frac{2\pi\omega P_c}{g R T} \int_0^{r_w} r^3 e^{\frac{\omega^2 r^2}{2 g R T}} (dr) \qquad (20)$$

$$\lambda = \frac{2\pi P_c}{\omega}\left[r^2 e^{\frac{\omega^2 r^2}{2gRT}} - \frac{2gRT}{\omega^2} e^{\frac{\omega^2 r^2}{2gRT}} \right]_0^{r_w} \qquad (21)$$

or,

$$\lambda = \frac{2\pi P_c}{\omega}\left[r_w^2 e^{\frac{\omega^2 r_w^2}{2gRT}} - \frac{2gRT}{\omega^2} e^{\frac{\omega^2 r_w^2}{2gRT}} + \frac{2gRT}{\omega^2} \right] \qquad (22)$$

Using equation (10) this may be simplified to,

$$\lambda = \frac{2\pi P_c r_w^2}{\omega}\left[e^{\frac{\gamma}{2} M_w^2} - \frac{2}{\gamma M_w^2}\left(e^{\frac{\gamma}{2} M_w^2} - 1\right)\right] \qquad (23)$$

Now the average angular momentum per pound of gas in the vortex cannot exceed the original angular momentum possessed by each pound of gas that formed it. Letting v_o be the entering tangential velocity and r_o the radius at which it enters,

$$v_o r_o = \frac{\lambda}{m} \qquad (24)$$

Using the angular momentum found in equation (23) and the mass from equation (16)

$$v_o r_o = \frac{\omega r_w^2\left[e^{\frac{\gamma}{2} M_w^2} - \frac{2}{\gamma M_w^2}\left(e^{\frac{\gamma}{2} M_w^2} - 1\right)\right]}{\left[e^{\frac{\gamma}{2} M_w^2} - 1\right]} \qquad (25)$$

which may be simplified to,

$$v_o r_o = \omega r_w^2 \left[\frac{e^{\frac{\gamma}{2} M_w^2}}{(e^{\frac{\gamma}{2} M_w^2} - 1)} - \frac{2}{\gamma M_w^2} \right] \qquad (26)$$

Equations (23) and (26) are valid only for the assumptions made, i.e., the flow is conforming to solid body rotation. Unfortunately, in the small annular converging section of the vortex tube it was not possible to determine this fact experimentally. It would have been necessary to take pressure and temperature data on the surface of the convergence cone, which would be extremely difficult. Also, the equations apply only to a solid vortex. They could, however, be altered for use in the annular area by integrating from the cone radius to the wall radius. But without data taken at the cone surface they could not be used.

An "efficiency of convergence" may be implied from equation (26) if defined in the following manner.

$$\eta = \frac{\omega r_w^2 \left[\frac{e^{\frac{\gamma}{2} M_w^2}}{(e^{\frac{\gamma}{2} M_w^2} - 1)} - \frac{2}{\gamma M_w^2} \right]}{v_o \quad r_o} \qquad (27)$$

If v_o and r_o are taken as the conditions existing as the flow leaves the vanes, equation (27) may be converted into terms of Mach number by expressing the velocity as,

$$v = \frac{M\sqrt{\gamma g R T_o}}{\sqrt{1 + \frac{\gamma-1}{2} M^2}} \qquad (28)$$

If the total temperature is assumed to remain constant, equation (27) becomes,

$$\eta = \frac{r_w}{r_v} \frac{M_w}{M_v} \sqrt{\frac{1 + \frac{\gamma-1}{2} M_v^2}{1 + \frac{\gamma-1}{2} M_w^2}} \left[\frac{e^{\frac{\gamma}{2} M_w^2}}{(e^{\frac{\gamma}{2} M_w^2} - 1)} - \frac{2}{\gamma M_w^2} \right] \qquad (29)$$

The assumption of constant total temperature was found to be well within the limits of experimental accuracy.

In order to make an experimental determination of the average angular momentum it would be necessary to probe the annular area radially at each station to obtain the average Mach number. This would require a redesign of the radial probes in order to obtain readings in the small annular area. Since this fact was not recognized until late in the investigation, time did not permit doing this.

In an effort to make some experimental determination of the angular momentum in the annular area from the wall data alone, the following analysis was made.

For an incremental annular area, (dA), the angular momentum is given by

$$(d\lambda) = v\, r\, \rho\, (dA) \qquad (30)$$

Using equation (6) and transposing,

$$\frac{d\lambda}{dA} = \frac{v\,r\,P}{g\,R\,T} \qquad \text{(31)}$$

The velocity may be expressed in terms of Mach number and total temperature from equation (28).

Eliminating v from equations (28) and (31),

$$\frac{d\lambda}{dA} = \frac{M\sqrt{\gamma\,g\,R\,T_o}}{\sqrt{1+\frac{\gamma-1}{2}M^2}} \quad \frac{r\,P}{g\,R\,T} \qquad \text{(32)}$$

But,

$$\frac{T_o}{T} = 1+\frac{\gamma-1}{2}M^2 \qquad \text{(33)}$$

So equation (32) becomes,

$$\frac{d\lambda}{dA} = \sqrt{\frac{\gamma}{g\,R\,T_o}}\; r\,P\,M\sqrt{1+\frac{\gamma-1}{2}M^2} \qquad \text{(34)}$$

When the wall data is used in equation (34) it will give the rate of change of angular momentum with respect to annular area at the wall. It is recognized that at any one station this value would probably be different at each radius of the annular area. Between stations, however, it should give some indication of how the angular momentum is changing. For convenience in computing equation (34), a curve was plotted of $M\sqrt{1+\frac{\gamma-1}{2}M^2}$ against M and is included as Figure 4.

RESULTS AND DISCUSSION

The results of the axial traverses for temperature and pressure are given in Tables I and II for the different weight flows. Curve 1 indicates that a vacuum existed in the vortex center at all weight flows and at all stations. A minimum pressure was found to occur at station 7 for each weight flow, although no significance could be attached to this fact. Vickrey, who did a limited amount of axial probing in his work, obtained curves very similar to these using a six-inch vortex tube of two-inch diameter. The indication is, therefore, that this point of minimum pressure is a function of the vortex tube geometry, and occurs at about the mid-length of the tube.

In Curve 2 it is seen that the vortex center temperature also has a tendency to reach a minimum point although at a station much closer to the convergence cone. This trend is just discernable in the 60-inch run, and becomes markedly apparent in the 80-inch run. It is interesting to note that at station 3 in the 80-inch run, a temperature of nearly five degrees Fahrenheit was recorded. This explains the interest that has been shown in the vortex tube as a refrigerating device, as mentioned in the Introduction of

this report. In this connection, it may be noted that considerable difficulty was encountered in taking the axial data due to the icing of the probes. If the probe was inserted well into the vortex tube when the compressor was started, ,so much ice would be formed on it as to seriously impair the flow or cause vibration of the probe. It was, therefore, necessary to position the probe at station 12 during the hour warm-up period of the compressor. After this length of time the supply air would reach a temperature high enough to prevent serious icing of the probes.

The static and total pressure data obtained at the vortex tube wall is presented in Tables I, II, III, and IV, and plotted in Curves 3 and 4. Since Mach number is a point function of total and static pressure, the Mach number was computed at each station from the above data and plotted in Curve 5. It may be seen from Curve 3 that the static pressure drops rapidly as the flow accelerates down the converg--nce cone. It reaches a minimum somewhere between stations 1 and 2, peaks at about station 3, and then falls off gradually through the rest of the vortex tube. The fact that the curve obtained for the 100-inch run does not follow the trend of the rest of the family, is probably due to shock phehomena and will be discussed further.

From Curve 4 it may be seen that the total pressure drops nearly linearly down the converging section, has a

tendency to level off as the flow leaves the tip of the convergence cone, and then drops off less steeply through the rest of the vortex tube. The tendency for the total pressure to level off as the flow leaves the convergence cone may be due to the fact that the flow is suddenly being released from the frictional effects of two wall surfaces to the frictional effect of only one wall surface. Thus, the rate of total pressure loss is momentarily reduced. The fact that this tendency is not so prominent in the 100-inch run is probably due to the supersonic flow present in this section.

From Curve 5 it may be seen that the Mach number rises very rapidly as the flow proceeds down the convergence cone. A peak is reached somewhere between stations 1 and 2 and the Mach number then drops off very rapidly. A Mach number of 1.009 was recorded at station 1. The curves indicate, however, that Mach numbers slightly higher than this are present between stations 1 and 2.

It may be well to note here that in computing the wall Mach number the static pressure was measured just at the wall, while the total pressure was measured at the point which gave the maximum reading. The distance from the wall that this maximum reading was obtained averaged about .02 inches, depending on the weight flow and station. This distance was probably very close to the boundary lay-

er thickness existing at the wall. It would be difficult to predict how the static pressure would vary in the boundary layer of a highly curvilinear flow. However, a Ser's disc probe was used to determine experimentally how the static pressure varied in this distance. It was found that in all cases the highest static pressure was present at the wall surface. Therefore, the values of Mach number found in this investigation are conservative inasmuch as they are all lower than the Mach number actually existing in the vortex tube. The discrepency, however, is not believed to exceed more than about 5 percent.

What actually happens as the flow becomes supersonic in a curvilinear flow is not readily apparent. It seems logical, however, that, as the flow is accelerating very rapidly down the convergence cone, it "winds" itself up with enough inertia to carry it into the supersonic region. It then seems probable that an infinite number of infinitesimal shocks occur from the vortex tube wall surface, which rapidly decelerates the flow but produces no abrupt changes such as found in normal shock phenomena. This could account for the fact that the 100-inch total pressure curve does not level off at the tip of the convergence cone as the other curves do, the losses occurring in the small shocks being enough to prevent it. The same applies to

the irregular shape of the 100-inch static pressure curve.

The fact that supersonic flow was produced in a vortex is interesting and, perhaps, of some practical value. For example, in the analysis of a thrust device designed to utilize vortex flow (as in the tail cone of a jet engine), Curve 3 would indicate that higher wall pressures could be obtained by not permitting the flow to become supersonic. This conclusion would apply, of course, only within the limited range of this investigation.

In an effort to determine if an equilibrium station existed in the vortex tube, equation (12) of the Theory was checked against the experimental data. Equation (12) was first plotted as shown in Curve 6. The experimental values of P_w/P_c and M_w were then plotted for each run. It may be seen from the plot that nowhere in the 40-inch run does the vortex come to an equilibrium station. In the 60-inch run, station 1 is close to equilibrium, while the following stations become farther removed from the theoretical curve. The same applies to the 80-inch run. Since no axial probing was done in the 100-inch run, it was not possible to determine if equilibrium existed, since the value of P_c was lacking. From the trend of the curves, however, it is very probable that an equilibrium plane existed close to station 1 for this run.

Both Vickrey and Zubko found equilibrium stations beyond the mid-length of the vortex tube. In their work the flow was introduced at the periphery. By viscous action the velocity of the inner radii was gradually increased, this process requiring a considerable length of the vortex tube before equilibrium was obtained. In this investigation, however, equilibrium was obtained, or perhaps it was already present, as the flow left the tip of the convergence cone. This would seem to indicate that the double frictional effect present in the converging annular area produces a rapid acceleration to an equilibrium condition. It is felt that this fact is worthy of note for use in the design of a vortex tube for any future investigations.

The values of $\frac{d\lambda}{dA}$ were computed from equation (34) as shown in the Tables and plotted in Curve 7. In computing these values it should be noted that the plenum chamber temperature was used as the total temperature. It was felt that this was justified since the total temperature probe indicated a discrepency of not more than six degrees from the plenum temperature.

As indicated in Curve 7, the value of $\frac{d\lambda}{dA}$ drops rapidly as the flow travels down the convergence cone, and then levels off in the constant diameter section of the

vortex tube. The value of $\frac{d\lambda}{dA}$, as mentioned previously, does not necessarily give a measure of the angular momentum at the station. It is simply the value of the change in angular momentum with respect to annular area at the wall surface of a specific station. It was hoped, however, that it would provide an indication of the trend in angular momentum change between stations. It seems logical that in the converging area, where the flow is subjected to the frictional effects of two surfaces, the loss in angular momentum would be greater than in the constant area section of the vortex tube. This trend is borne out by the curves of Curve 7, although this still does not justify the assumption that $\frac{d\lambda}{dA}$ will vary between stations in exactly the same way as the angular momentum.

The convergence efficiency was computed from equation (29) and is plotted in Curve 8. Since the equation demands that the flow be in equilibrium, the efficiency was found only for the station that was closest to equilibrium in each run. Station 1 was used in each case, although in the 40-inch run equilibrium did not appear to exist. From Curve 8 it may be seen that the convergence efficiency rises with increased wall velocities (i.e., increased supply pressure). This seems rather unusual, but no explanation can be offerred.

As another check on the legitimacy of using $\frac{d\lambda}{dA}$ as an indicator to angular momentum, a $\frac{d\lambda}{dA}$ "efficiency" was computed by dividing the value found at the equilibrium station by the entering value found at the vanes. The result is plotted in Curve 8, and is surprisingly close to the actual convergence efficiency.

The results of the tests run with the convergence cone removed from the vortex tube are presented in Tables V, VI, and VII and plotted in Curves 9 to 13. A 40-inch run was not made since it was doubtful if an equilibrium station would be found at this weight flow.

A comparison of Curve 9 with Curve 3 shows that the static pressure behaves in the same manner when the convergence cone is removed, although the 100-inch curve does not show an irregular shape. This is probably due to the fact that supersonic wall velocities were not attained, as will be seen.

The total pressure curves, Curve 10, are similar to those obtained previously, Curve 4. The loss in total pressure down the converging section appears to be greater, however, with the convergence cone removed. Logically it would seem that the reverse should be true, since the flow feels a double frictional effect with the convergence cone present. With the cone removed, however, the flow "fills

in" behind the face of the vortex valve. Then, by viscous action, it performs the work of gradually accelerating this inner air. This produces an apparent loss of total pressure at the wall, which is evidently more than enough to offset the loss in total pressure due to friction when the convergence cone is present.

A comparison of Curves 11 and 5 shows the effect of the convergence cone on wall Mach number. It may be seen that with the cone removed considerably lower Mach numbers are obtained at the wall. This is probably caused by two effects. First, the "filling in" process described above would tend to lower the Mach number. Secondly, in subsonic flow the effect of friction is to increase Mach number, so that with the convergence cone present increased Mach number would be expected from the larger amount of friction which is present. The shape of the curves of Curve 11 would seem to indicate that the "filling in" process first lowers the Mach number. Then, as the inner air is brought into rotation, the Mach number begins to increase. The fact that the 100-inch curve shows a continuous drop in Mach number in the converging section is not readily explainable. It may be that the higher velocities present require a longer length for the "filling in" process to be completed. This would be especially true if the axial component of flow is increased greatly with increased entering velocity.

Curves 12 and 13 are plots of $\frac{d\lambda}{dA}$ and convergence efficiency respectively. The curves of $\frac{d\lambda}{dA}$ are very similar to those found with the convergence cone present, Curve 7, although the values are somewhat lower. In computing the values of convergence efficiency, it was assumed that station 1 was in equilibrium as in the previous runs. This fact cannot be proven, however, since no center probing was done with convergence cone removed. However, due to the similarity of the data it is believed that this is a fair approximation. From Curve 13 it may be seen that convergence efficiencies are lower with the convergence cone removed, and that the values of $(\frac{d\lambda}{dA})_1 / (\frac{d\lambda}{dA})_v$ are fairly close to the convergence efficiencies. The fact that lower efficiencies occur with the cone removed is probably due to the loss in angular momentum as the flow accelerates the inner air in the converging section.

The Mach number at the vanes was computed from the known values of area, weight flow, and total temperature, and the static pressure measured at the vanes. In computing the area it was assumed that the flow left the vanes in the same direction as the vane angle, i.e., at ten degrees to the peripheral tangent.

CONCLUSIONS

The results of this investigation indicate that it is possible to obtain supersonic velocities in a vortex which is made to converge down an annular passage. If the vortex flow is induced at the periphery, greater velocities will be produced if the flow converges down a solid cone than if it converges with no cone present.

It was shown that convergence of a vortex down an annular passage tends to bring the flow to a condition of equilibrium much more rapidly than if it were introduced at the periphery of a constant area tube.

The loss in angular momentum of the flow is very great as the vortex converges down an annular passage. However, an even greater loss in angular momentum is indicated if a convergence cone is not present.

RECOMMENDATIONS

In future investigations into vortex flow it is recommended that the "self-adjusting" nose cone be given further study. It is firmly believed that this device answers a great need in experimental vortex investigations. The discharge end of the vortex tube could be carefully traversed for static pressure over the range of weight flows to be used. The nose cone could then be made with the exact taper required by the pressure gradient. One nose cone could probably cover a wide range of weight flows satisfactorily, although it might be necessary to construct several different cones to cover the entire range, especially if the character of the flow was greatly changed as was done in this investigation by the removal of the convergence cone.

The author believes that a more extensive investigation should be made of the angular momentum in the converging section of the vortex tube. To do this properly the annular area would have to be probed radially, and would require the design and construction of very small probes.

In future investigations of a converging vortex it

is felt that the validity of the theory could be checked more closely if the vortex were brought into equilibrium just before it converges. A convergence section similar to the one used in this investigation could be employed to bring the vortex into equilibrium in as short a length as possible. The flow would then enter an additional convergence (or divergence) section where its characteristics could be studied.

BIBLIOGRAPHY

(1) Bailey, N. P. - "Performance of a Vortex Valve", General Electric Research Laboratory, Schenectady, New York, Data Folder No. 45266, May 1943

(2) Corr, J. E. - "The Vortex Tube", General Electric Research Laboratory, Schenectady, New York, Data Folder No. 45289, July 1948

(3) Vickrey, W. C. - "Vortex Flow in an Actual Gas", a graduate Thesis prepared in the Department of Mechanical Engineering, Rensselaer Polytechnic Institute, Troy, New York, May, 1948

(4) Zubko, L. M. - "Characteristics of a Vortex in an Actual Gas", a graduate Thesis prepared in the Department of Mechanical Engineering, Rensselaer Polytechnic Institute, Troy, New York, January, 1949

SAMPLE CALCULATIONS

To illustrate the manner in which the experimental data was reduced to the form presented here, the computations for the 60-inch run, Station 1, will be detailed.

Barometer = 30.08 "Hg. T_{op} = 112°F = 572°R

P_w = 9.05 "Hg gage = 9.05 + 30.08 = 39.13 "Hg.

P_o = 32.60 "Hg. gage = 32.60 + 30.08 = 62.68 "Hg. Abs.

P_c = -6.30 "Hg. gage = -6.30 + 30.08 = 23.78 "Hg. Abs.

T_c = -.08 M_v = 29.2°F = 488.6°R

$$\frac{P_o}{P_w} = \frac{62.68}{39.13} = 1.602$$

From Mach tables, M_w = .850

$$\frac{P_w}{P_c} = \frac{39.13}{23.78} = 1.644$$

From Figure 4, $M\sqrt{1 + \frac{\gamma-1}{2}M^2} = .908$

From equation (34)

$$\frac{d\lambda}{dA} = \sqrt{\frac{1.395}{(32.2)(53.3)(572)}\,(.6345)(39.13)(70.73)(.908)}$$

$$= 1.902 \quad \frac{\text{lb-sec-in}}{\text{ft}^3}$$

The value of M_v was found to be .663 for this run.

r_v = 1.375 in.

So from equation (29),

$$\eta = \frac{(.6345)}{(1.375)}\,\frac{(.850)}{(.663)}\sqrt{\frac{1+\frac{\gamma-1}{2}(.663)^2}{1+\frac{\gamma-1}{2}(.850)^2}\left[\frac{e^{\frac{\gamma}{2}(.85)^2}}{(e^{\frac{\gamma}{2}(.85)^2}-1)}-\frac{2}{\gamma(.85)^2}\right]}$$

$$= .303$$

At the vanes, $\frac{d\lambda}{dA} = 4.92$. So,

$$\left(\frac{d\lambda}{dA}\right)_l \Big/ \left(\frac{d\lambda}{dA}\right)_v = \frac{1.902}{4.92} = .387$$

The calculations with the convergence cone removed were made in an idential menner.

TABLE I

Station	P_w "Hg.g	P_w Hg.abs.	P_o Hg.g	P_o Hg.abs.	P_c Hg.g	P_c Hg.abs.	Milli-volt	T_c °F
V	22.00	51.66						
A	20.20	49.86						
B	17.00	46.06						
C	12.40	42.06						
1	7.55	37.21	22.10	51.76	-5.40	24.26	.06	34.1
2	8.35	38.01	18.75	48.41	-5.60	24.06	.06	34.1
3	9.35	39.01	16.20	45.86	-5.70	23.96	.08	34.8
4	8.00	37.66	15.10	44.76	-6.00	23.66	.10	35.5
5	7.70	37.36	14.05	43.71	-6.10	23.56	.12	36.2
6	6.70	36.36	12.95	42.61	-6.30	23.36	.14	36.8
7	6.10	35.76	11.40	41.06	-6.50	23.16	.16	37.5
8	5.00	34.66	11.00	40.66	-6.30	23.36	.22	39.6
9	4.60	34.26	10.50	40.16	-6.30	23.36	.31	42.7
10	4.70	34.36	9.85	39.51	-6.10	23.56	.41	46.1
11	4.30	33.96	8.95	38.61	-6.10	23.56	.50	49.4
12	3.90	33.56	8.20	37.86	-5.85	23.81		

TABLE I Cont'd.

Station	P_o/P_w	M_w	P_w/P_c	$M\sqrt{1+\frac{\gamma-1}{2}M^2}$	$\frac{d\lambda}{dA}$
V		.590		.610	3.66
A					
B					
C					
1	1.390	.703	1.532	.739	1.470
2	1.278	.596	1.580	.616	1.252
3	1.173	.483	1.630	.497	1.040
4	1.189	.504	1.591	.520	1.000
5	1.171	.481	1.584	.496	.992
6	1.172	.483	1.556	.497	.966
7	1.149	.451	1.542	.465	.890
8	1.172	.483	1.485	.497	.922
9	1.172	.483	1.469	.497	.910
10	1.150	.453	1.458	.467	.860
11	1.138	.434	1.441	.445	.808
12	1.130	.423	1.409	.433	.778

P_{op1} 42.3 "hg.g
P 1.75 "hg
P_{op2} 40.0 "hg.g
Bar. 29.66 "hg
T_{op} 112°F
W .1115 lb/sec

$$\eta = \frac{\left(\frac{d\lambda}{dA}\right)_1}{\left(\frac{d\lambda}{dA}\right)_v} = .276 \div .402$$

TABLE II

Station	P_w "hg.g.	P_w "hg.abs.	P_o hg.g.	P_o hg.abs.	P_c hg.g.	P_c hg.abs.	Milli-volts	T_c °F
V	39.45	61.53						
A	29.90	59.98	40.80	70.88				
B	26.50	56.58	37.60	67.68				
C	18.80	48.88	32.80	62.88				
1	9.05	39.13	32.60	62.68	-6.30	23.78	-.08	29.2
2	10.95	41.03	27.75	57.83	-6.65	23.43	-.12	27.9
3	12.90	42.98	23.00	53.08	-6.85	23.23	-.10	28.5
4	11.60	41.68	21.80	51.88	-7.25	22.83	-.09	28.9
5	11.00	41.08	20.95	51.03	-7.85	22.23	-.08	29.2
6	10.20	40.28	18.70	48.78	-8.05	22.03	-.08	29.2
7	9.30	39.38	17.20	47.28	-8.10	21.98	0	32
8	8.30	38.38	15.70	45.78	-8.00	22.08	.08	34.8
9	7.60	37.68	15.10	45.18	-7.90	22.18	.16	37.5
10	6.90	36.98	14.25	44.33	-7.75	22.33	.24	40.4
11	6.50	36.58	12.85	42.93	-7.60	22.48	.28	41.7
12	5.60	35.68	11.90	41.88	-6.75	23.33	.41	46.2

TABLE II Cont'd.

Station	P_o/P_w	M_w	P_w/P_c	$M\sqrt{1+\frac{\gamma-1}{2}M^2}$	$\frac{d\lambda}{dA}$
V		.663		.694	4.92
A	1.181	.494		.509	3.55
B	1.195	.511		.528	2.58
C	1.288	.613		.636	1.77
1	1.602	.850	1.644	.908	1.902
2	1.409	.718	1.750	.883	1.620
3	1.234	.558	1.850	.596	1.371
4	1.242	.566	1.821	.585	1.292
5	1.241	.565	1.846	.584	1.270
6	1.211	.531	1.828	.550	1.175
7	1.200	.518	1.791	.532	1.111
8	1.192	.507	1.738	.522	1.061
9	1.198	.515	1.700	.530	1.060
10	1.199	.516	1.656	.531	1.041
11	1.172	.483	1.620	.499	.967
12	1.171	.481	1.531	.501	.946

P_{op_1} 62.7 "hg.g.
P 2.50 "hg
P_{op_2} 60.0 "hg.g.
Bar 30.08 "hg.
T_{op} 112°F
W .1500 lb/sec

$$\eta = \left(\frac{d\lambda}{dA}\right)_l \div \left(\frac{d\lambda}{dA}\right)_v$$

η = .303

= .387

TABLE III

Station	P_w "hg.g	P_w "hg.abs.	P_o "hg.g	P_o "hg.abs.	P_c "hg.g.	P_c "hg.abs.	Milli-volts	T_c °F
V	40.30	70.36						
A	38.55	68.61	54.00	84.06				
B	33.95	64.01	49.30	79.36				
C	23.30	53.36	44.20	74.26				
1	10.30	40.36	43.30	73.36	-8.40	21.66	-.48	15.4
2	13.20	43.26	36.35	66.41	-8.55	21.51	-.70	7.7
3	17.35	47.41	30.75	60.81	-8.90	21.16	-.76	5.6
4	15.05	45.11	28.00	58.06	-9.35	20.71	-.68	8.4
5	15.85	45.91	26.05	56.11	-9.55	20.51	-.59	11.5
6	14.15	44.21	25.00	55.06	-9.90	20.16	-.50	14.6
7	12.35	42.41	21.55	51.61	-10.10	19.96	-.42	17.5
8	12.10	42.16	19.90	49.96	-10.20	19.86	-.36	19.5
9	10.55	40.61	18.50	48.56	- 9.85	20.21	-.30	21.6
10	9.50	39.56	18.10	48.16	- 9.95	20.11	-.19	25.4
11	9.15	39.21	16.60	46.66	- 9.20	20.86	-.09	28.8
12	7.90	37.96	15.20	45.26	- 8.85	21.21		

TABLE III Cont'd.

Station	P_o/P_w	M_w	P_w/P_c	$M\sqrt{1+\frac{\gamma-1}{2}M^2}$	$\frac{d\lambda}{dA}$
V		.707		.741	6.00
A	1.223	.545		.563	4.50
B	1.238	.562		.582	3.21
C	1.392	.705		.740	2.24
1	1.818	.966	1.861	1.048	2.24
2	1.532	.806	2.010	1.023	2.14
3	1.283	.608	2.240	.586	1.491
4.	1.308	.633	2.180	.640	1.526
5	1.222	.544	2.235	.563	1.370
6	1.242	.566	2.200	.585	1.378
7	1.220	.541	2.120	.577	1.280
8	1.174	.485	2.120	.500	1.120
9	1.193	.509	2.010	.541	1.158
10	1.218	.539	1.966	.556	1.158
11	1.190	.505	1.880	.480	1.022
12.	1.192	.507	1.791	.522	1.106

P_{op_1} 40.7 psig
P 3.10 "hg
P_{op_2} 39.4 psig
Bar 30.06 "hg.
T_{op} 112°F
W .1840 lb/sec

$$\eta = \left(\frac{d\lambda}{dA}\right)_1 \div \left(\frac{d\lambda}{dA}\right)_v$$

η = .332

= .377

TABLE IV

Station	P_w hg.g	P_w hg.abs.	P_o hg.g	P_o hg.abs.
V	49.85	79.79		
A	47.60	77.54		
B	41.25	71.19	60.00	89.94
C	40.10	60.04	55.60	85.51
1	13.15	43.09	52.50	82.44
2	14.85	44.79	44.30	74.24
3	16.25	46.19	36.15	66.09
4	16.35	46.29	33.75	63.69
5	16.35	46.29	30.35	60.29
6	15.90	45.84	30.85	60.79
7	13.55	43.49	25.65	55.59
8	13.15	43.09	25.05	54.99
9	11.85	41.79	23.90	53.84
10	9.65	39.59	22.10	52.04
11	11.25	40.19	22.10	52.04
12	9.15	39.09	20.15	50.09

TABLE IV CONT'd.

Station	Po/Pw	M_w	$M\sqrt{1+\frac{\gamma-1}{2}M^2}$	$\frac{d\lambda}{dA}$
V		.739	.778	7.15
A				
B	1.263	.588	.609	3.74
C	1.424	.730	.768	2.63
1	1.910	1.009	1.10	2.52
2	1.658	.883	.948	2.26
3	1.431	.735	.783	1.920
4	1.378	.693	.726	1.790
5	1.320	.627	.652	1.600
6	1.328	.650	.680	1.655
7	1.271	.593	.613	1.415
8	1.274	.600	.620	1.420
9	1.288	.613	.638	1.415
10	1.313	.637	.664	1.395
11	1.294	.619	.642	1.370
12	1.282	.607	.630	1.310

P_{op1} 50.3 psig
3.75 "Hg.
P_{op2} 49.0 psig
Bar 29.94 "Hg.
T_{op} 120°F
W .2175 lb/sec

$$\eta = \frac{}{\left(\frac{d\lambda}{dA}\right)_1 \div \left(\frac{d\lambda}{dA}\right)_v} = .338 = .352$$

TABLE V

Station	P_w "Hg.g	P_w "Hg.abs.	P_o "Hg.g	P_o "Hg.abs.
V	25.90	55.83		
A	25.50	55.43	36.70	66.63
B	19.20	49.13	27.60	57.53
C	11.30	41.23	20.45	50.38
1	5.90	35.83	15.10	45.03
2	6.05	35.98	13.05	42.98
3	6.95	36.88	11.60	41.53
4	6.45	36.38	10.80	40.73
5				
6	5.65	35.58	9.60	39.53
7				
8	5.10	35.03	8.95	38.88
9				
10	4.35	34.28	8.20	38.13
11				
12	3.65	33.58	7.40	37.33

TABLE V Cont'd.

Station	P_o/P_w	M_w	$M\sqrt{1+\frac{\gamma-1}{2}M^2}$	$\frac{d\lambda}{dA}$
V		.752	.793	5.10
A	1.203	.521	.539	3.46
B	1.170	.480	.493	2.09
C	1.221	.543	.560	1.315
1	1.255	.580	.600	1.142
2	1.194	.510	.526	1.009
3	1.127	.418	.427	.839
4	1.120	.407	.415	.800
5				
6	1.116	.400	.406	.767
7				
8	1.111	.392	.400	.757
9				
10	1.111	.392	.400	.729
11				
12	1.111	.392	.400	.714

P_{op_1} 31.0 psig
P 3.7 "hg
P_{op_2} 60 "hg.g
Bar 29.93 "hg.
T_{op} 121°F
W = .1550 lb/sec

$$\eta = \frac{\left(\frac{d\lambda}{dA}\right)_1}{\left(\frac{d\lambda}{dA}\right)_v} = .186 \div .224$$

TABLE VI

Station	P_w "Hg.g	P_w "Hg.abs.	P_o "Hg.g	P_o "hg.abs.
V	32.65	62.58		
A	31.90	61.83	46.20	76.13
B	24.30	54.23	35.60	65.53
C	14.50	44.43	26.70	56.63
1	7.30	37.23	19.65	49.58
2	7.70	37.63	17.40	47.33
3	8.90	38.83	15.00	44.93
4	8.15	38.08	14.00	43.93
5				
6	7.10	37.03	12.40	42.33
7				
8	6.50	36.43	11.50	41.43
9				
10	5.70	35.63	10.50	40.43
11				
12	4.55	34.48	9.65	39.58

TABLE VI Cont'd.

Station	P_o/P_w	M_w	$M\sqrt{1+\frac{\gamma-1}{2}M^2}$	$\frac{d\lambda}{dA}$
V		.798	.847	6.21
A	1.231	.554	.472	3.40
B	1.210	.530	.547	2.56
C	1.278	.604	.627	1.585
1	1.331	.654	.684	1.350
2	1.257	.582	.602	1.201
3	1.155	.459	.470	.969
4	1.151	.454	.465	.940
5				
6	1.142	.440	.462	.927
7				
8	1.135	.430	.451	.872
9				
10	1.13[illegible]	.426	.436	.825
11				
12	1.147	.448	.460	.842

P_{op_1} 39.4 psig
P 3.35 " Hg.
P_{op_2} 37.9 psig
Bar 29.93 "hg.
T_{op} 121°F
W = .1849 lb/sec

$$\eta = \left(\frac{d\lambda}{dA}\right)_1 \div \left(\frac{d\lambda}{dA}\right)_v$$

= .196

= .217

TABLE VII

Station	P_w "Hg.g	P_w "Hg.abs.	P_o "Hg.g	P_o "Hg.abs.
V	40.60	70.55		
A	39.60	69.55	57.30	87.25
B	30 .80	60.75	42.00	71.95
C	18.60	48.55	35.10	65.05
1	8.10	38.05	25.70	55.65
2	9.25	39.20	22.50	52.45
3	11.45	41.40	19.60	49.55
4	10.50	40.45	18 .10	48.05
5				
6	9.15	39.10	16.30	46.25
7				
8	8.40	38.35	14.95	44.90
9				
10	7.20	37.15	13.45	43.40
11				
12	5.90	35.85	12.20	42.15

TABLE VII Cont'd.

Station	P_o/P_w	M_w	$M\sqrt{1+\frac{\gamma-1}{2}M^2}$	$\frac{d\lambda}{dA}$
V		.870	.931	7.56
A	1.253	.576	.595	4.83
B	1.183	.496	.510	2.68
C	1.340	.429	.439	1.211
1	1.465	.760	.801	1.620
2	1.338	.660	.690	1.439
3	1.199	.516	.531	1.166
4	1.188	.503	.520	1.118
5				
6	1.182	.495	.510	1.060
7				
8	1.170	.480	.494	1.003
9				
10	1.168	.477	.490	.966
11				
12	1.175	.486	.501	.955

P_{op_1} 49.6 psig
P_{op_1} 4.0 "hg.
P_{op_2} 47.6 psig
Bar 29.95 "hg
T_{op} 120°F
W_{op} = .231 lb/sec

$$\eta = \left(\frac{d\lambda}{dA}\right)_1 \div \left(\frac{d\lambda}{dA}\right)_v$$

η = .217

= .214

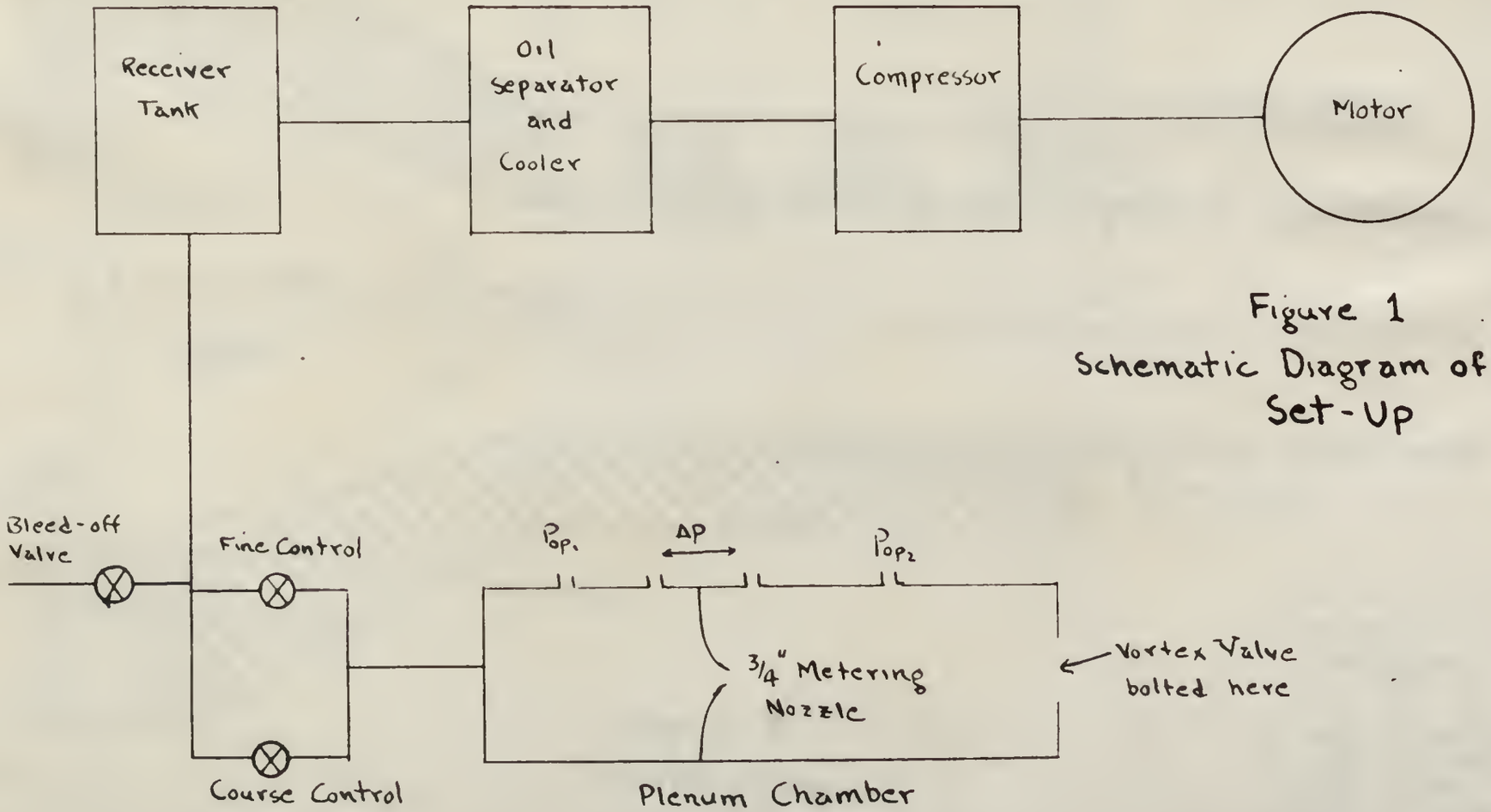

Figure 1
Schematic Diagram of Test Set-Up

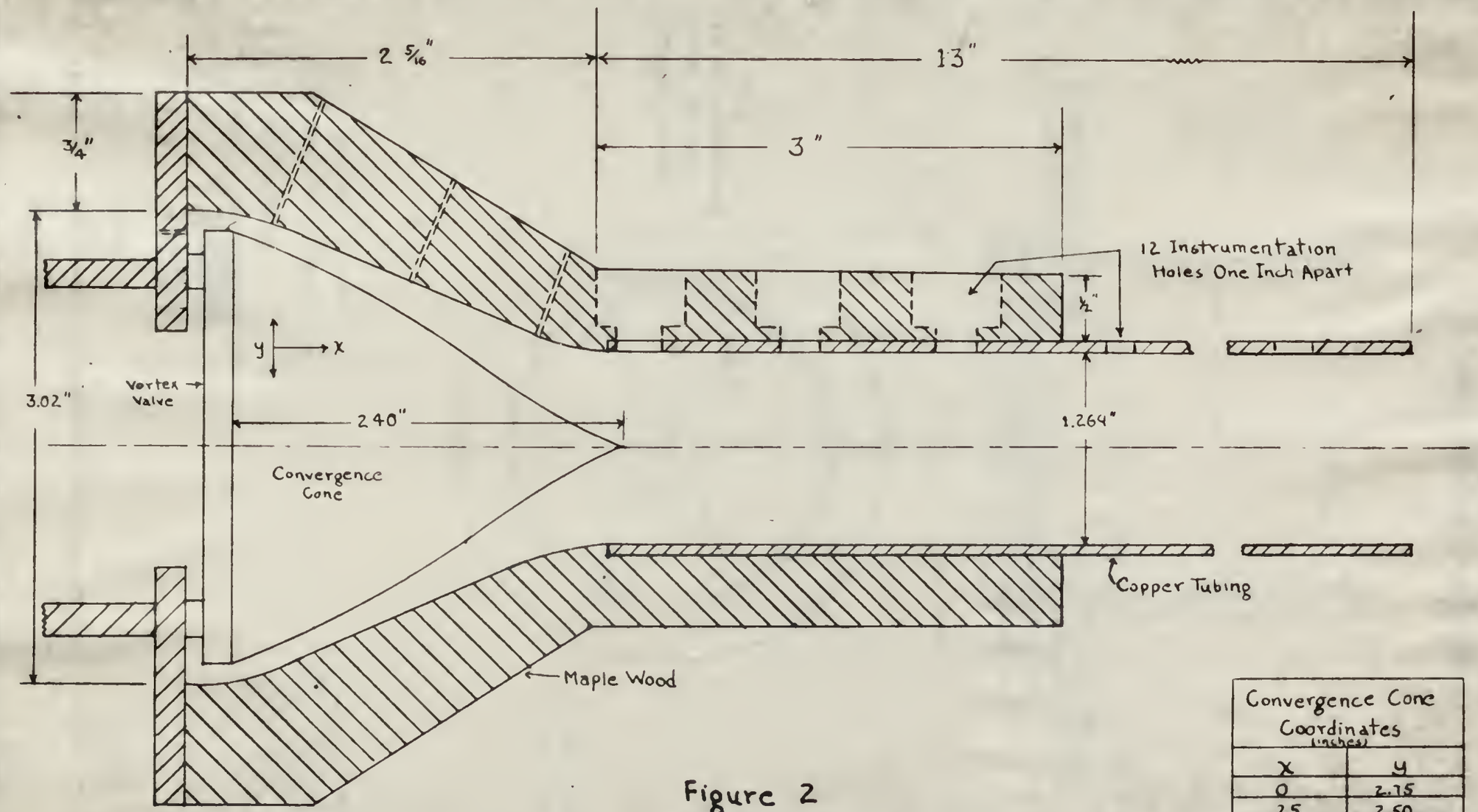

Figure 2
Vortex Tube

Convergence Cone Coordinates (inches)	
X	Y
0	2.75
.25	2.50
.50	2.25
.75	1.99
1.00	1.73
1.25	1.46
1.50	1.14
1.75	.75
2.00	.40
2.25	.12
2.40	0

Figure 3
Vortex Valve Assembly

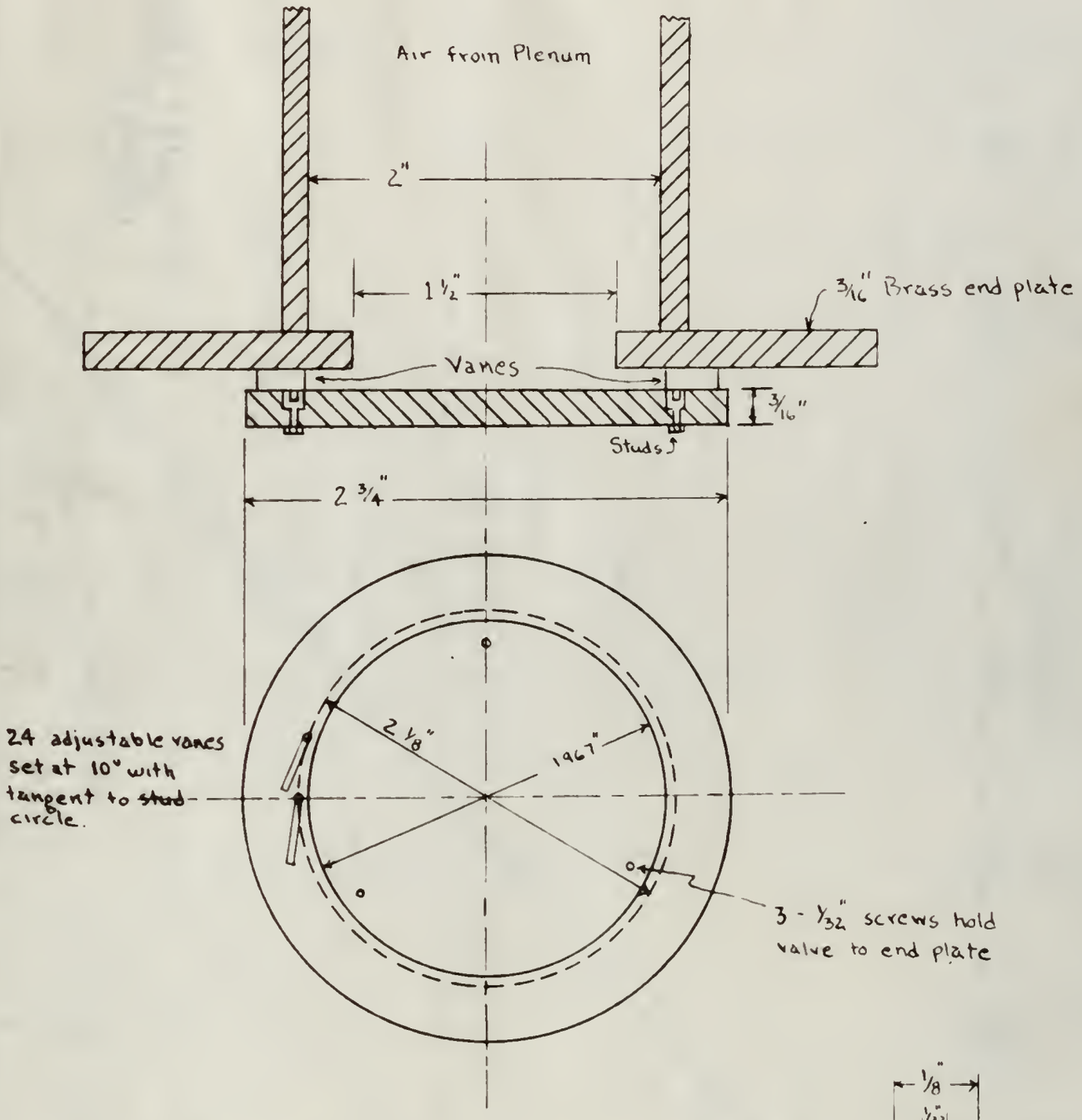

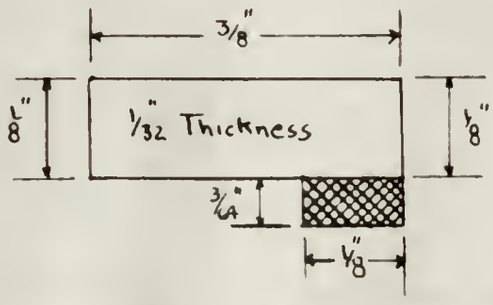

Vane Detail

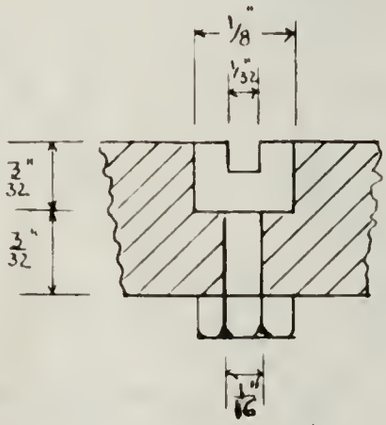

Stud Detail

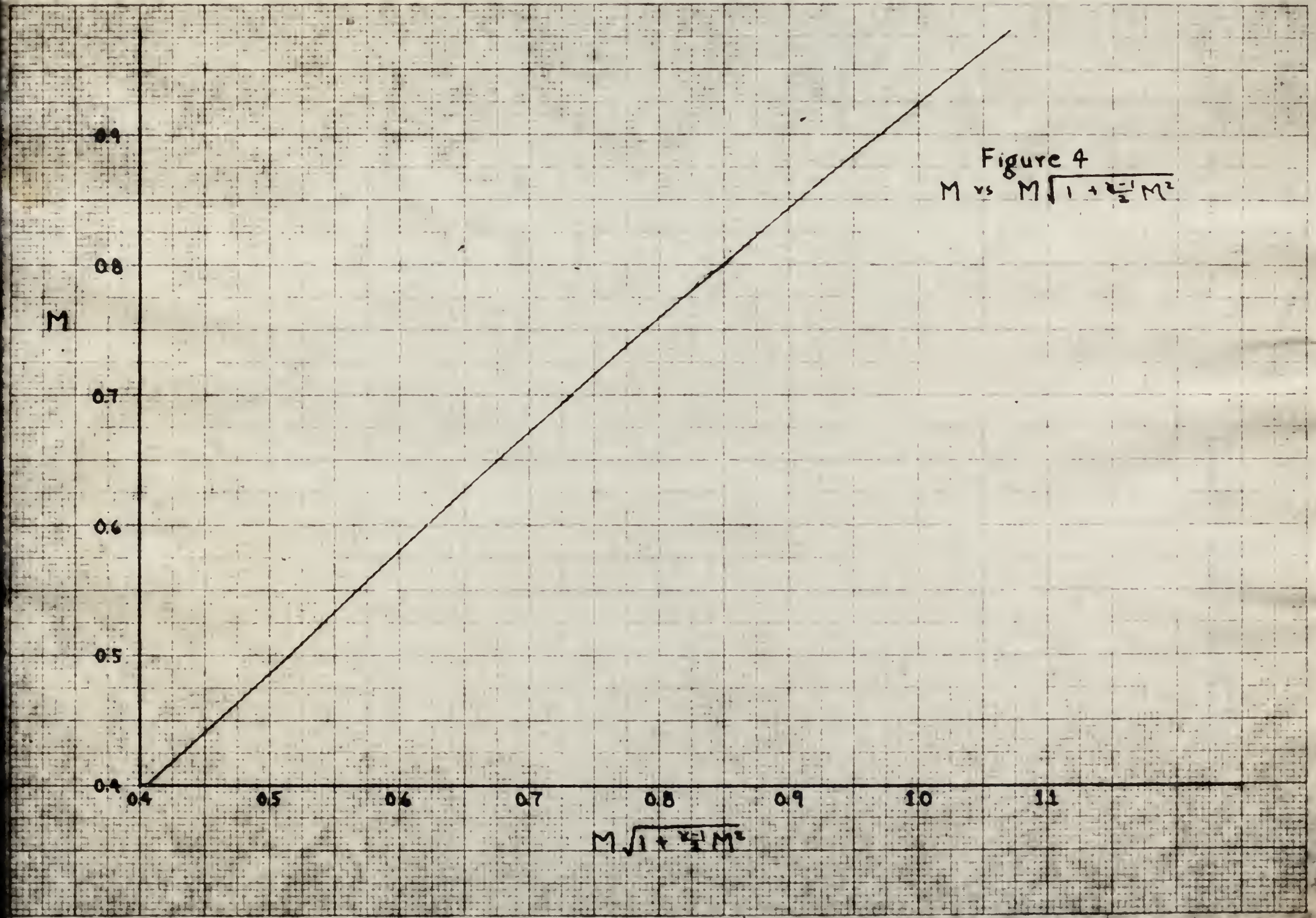

Figure 4
M vs $M\sqrt{1+\frac{\gamma-1}{2}M^2}$

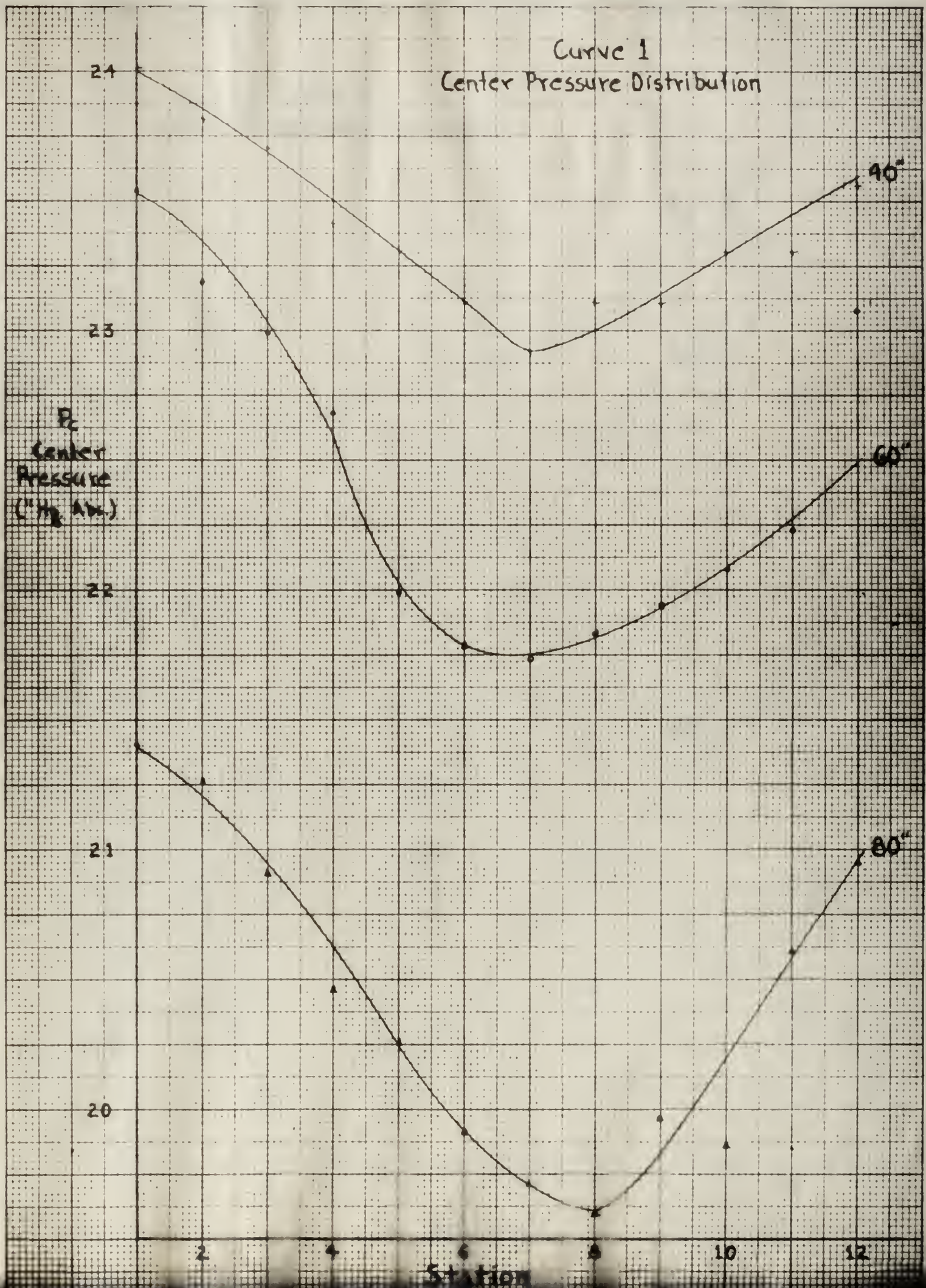
Curve 1
Center Pressure Distribution
24
23
22
21
20
P_c Center Pressure ("H_g Abs.)
40°
60°
80°
2
4
6
8
10
12
Station

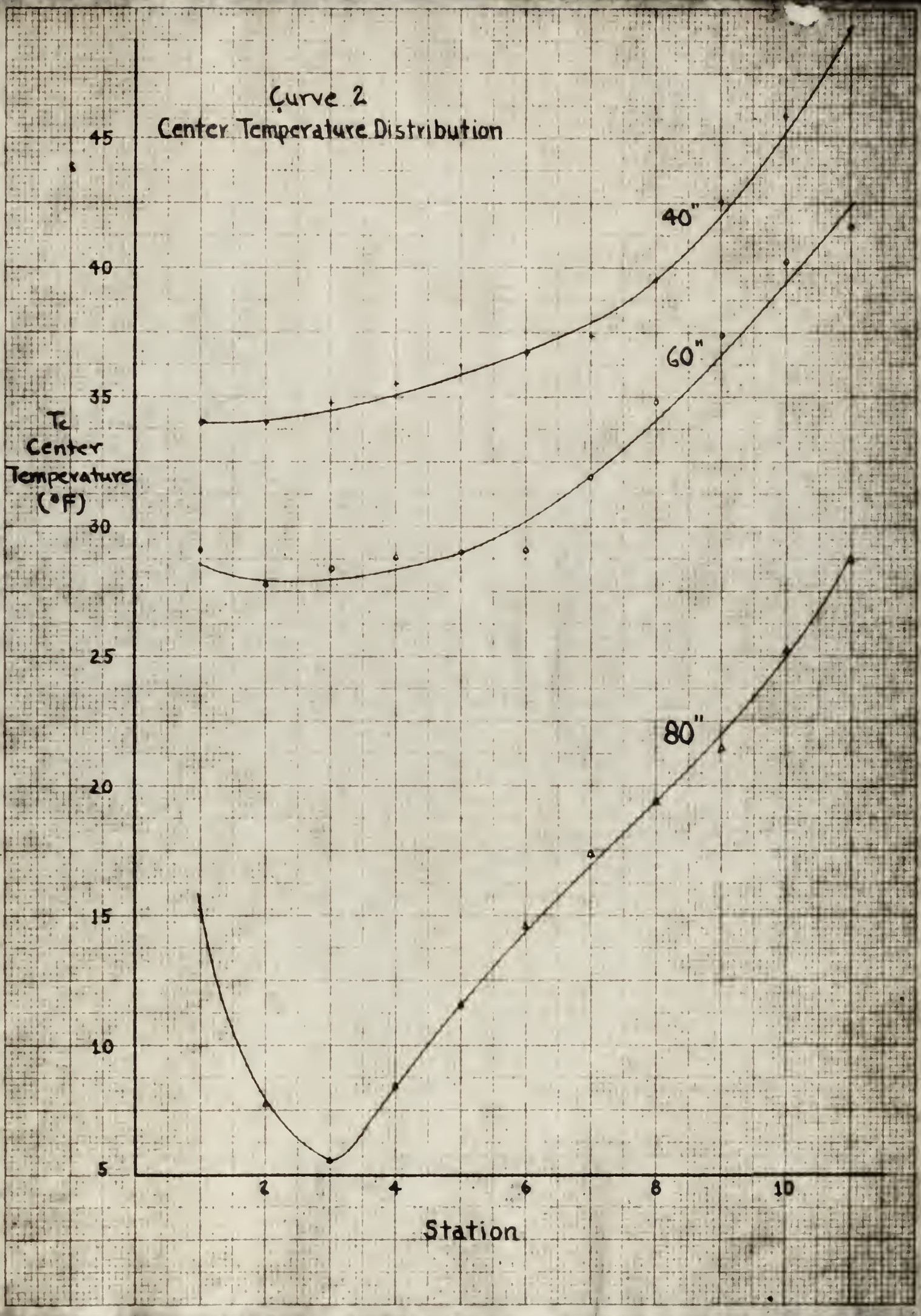
Curve 2
Center Temperature Distribution
45
40
35
30
25
20
15
10
5
Te
Center
Temperature
(°F)
40"
60"
80"
2
4
6
8
10
Station

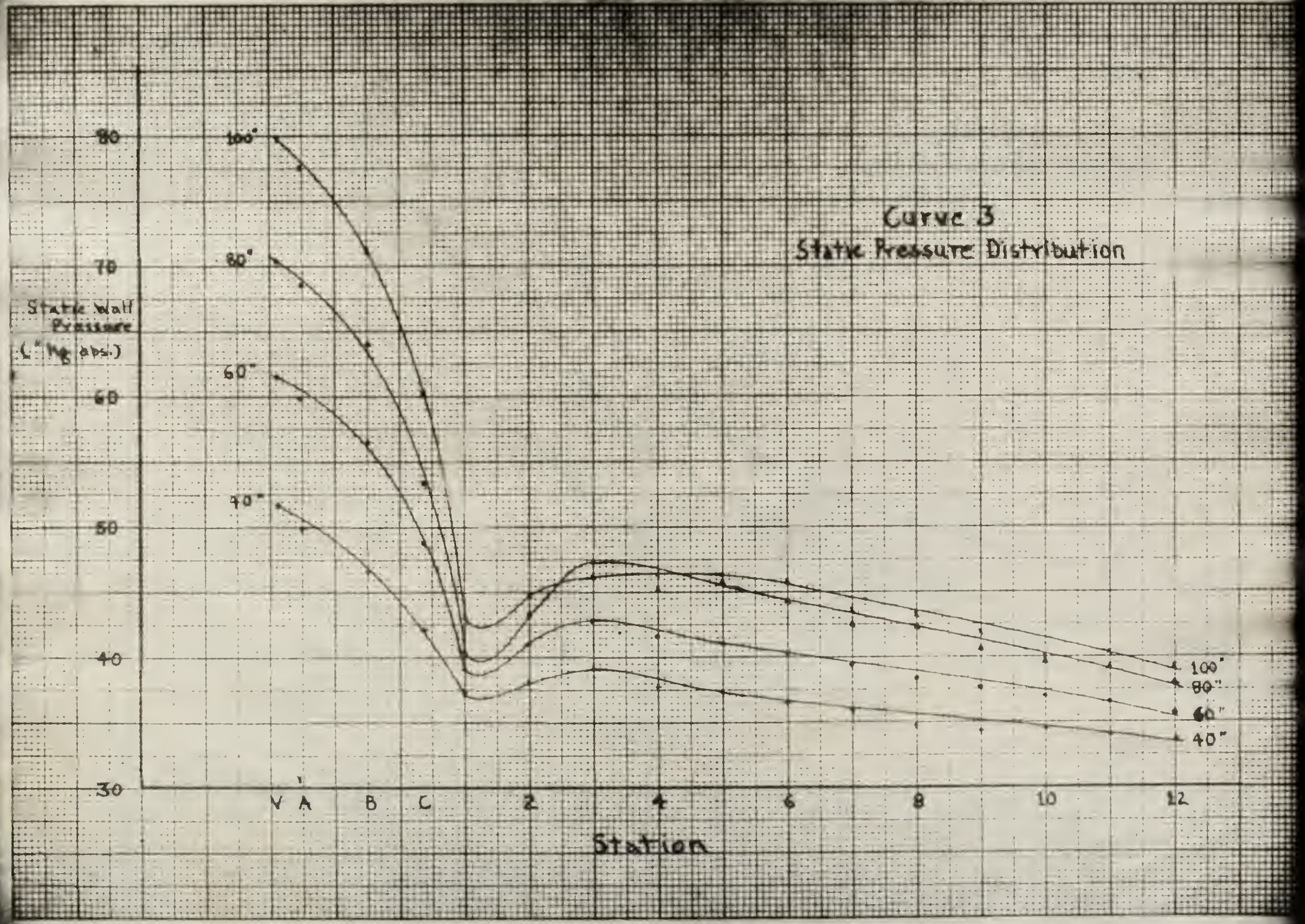
Curve 3
Static Pressure Distribution
Static Wall Pressure (" Hg abs.)
80
70
60
50
40
30
100"
80"
60"
40"
V
A
B
C
2
4
6
8
10
12
Station

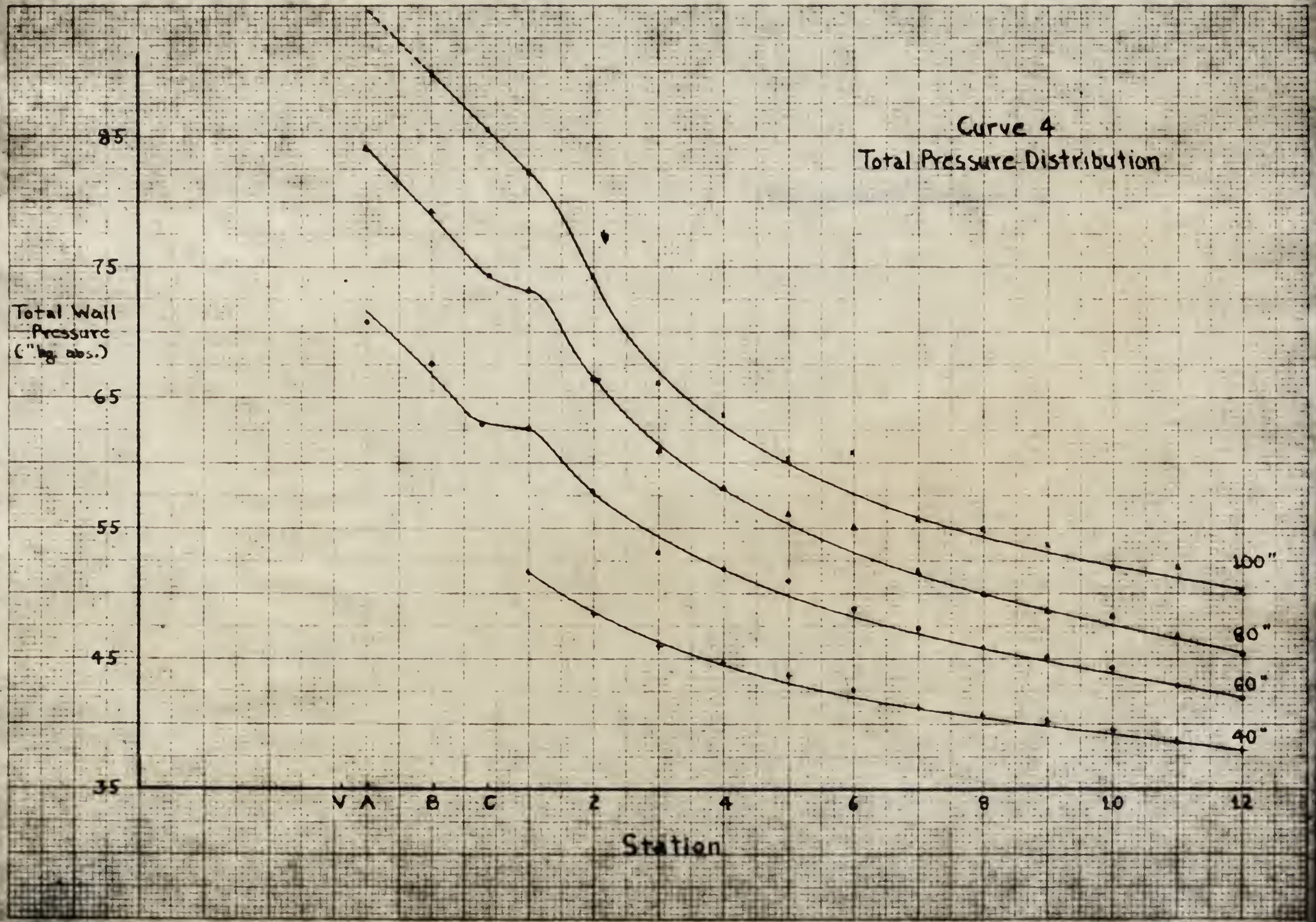
Curve 4
Total Pressure Distribution
Total Wall Pressure ("hg abs.)
85
75
65
55
45
35
V
A
B
C
2
4
6
8
10
12
Station
100"
80"
60"
40"

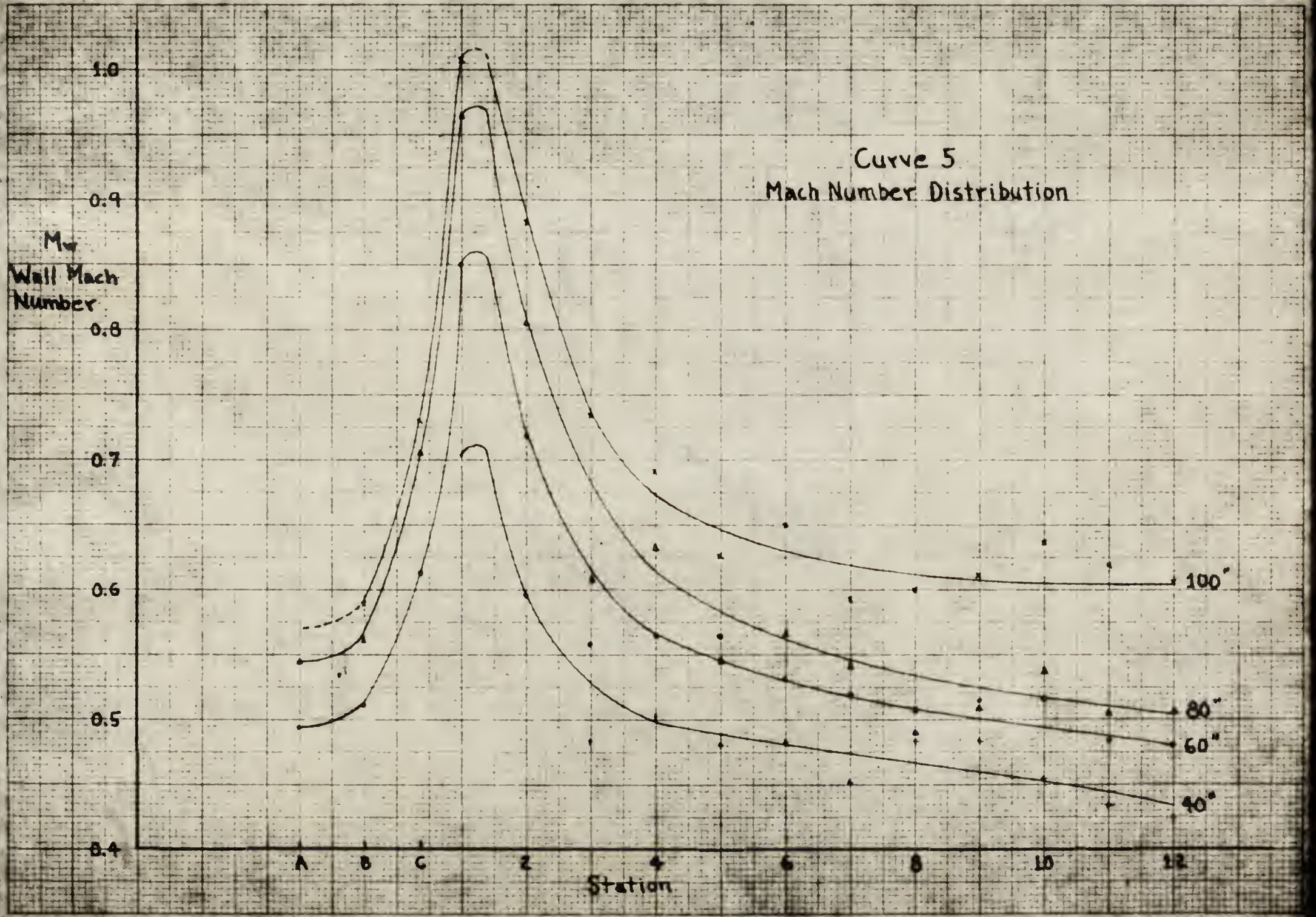
Curve 5
Mach Number Distribution
M_w
Wall Mach Number
1.0
0.9
0.8
0.7
0.6
0.5
0.4
A
B
C
2
4
6
8
10
12
Station
100"
80"
60"
40"

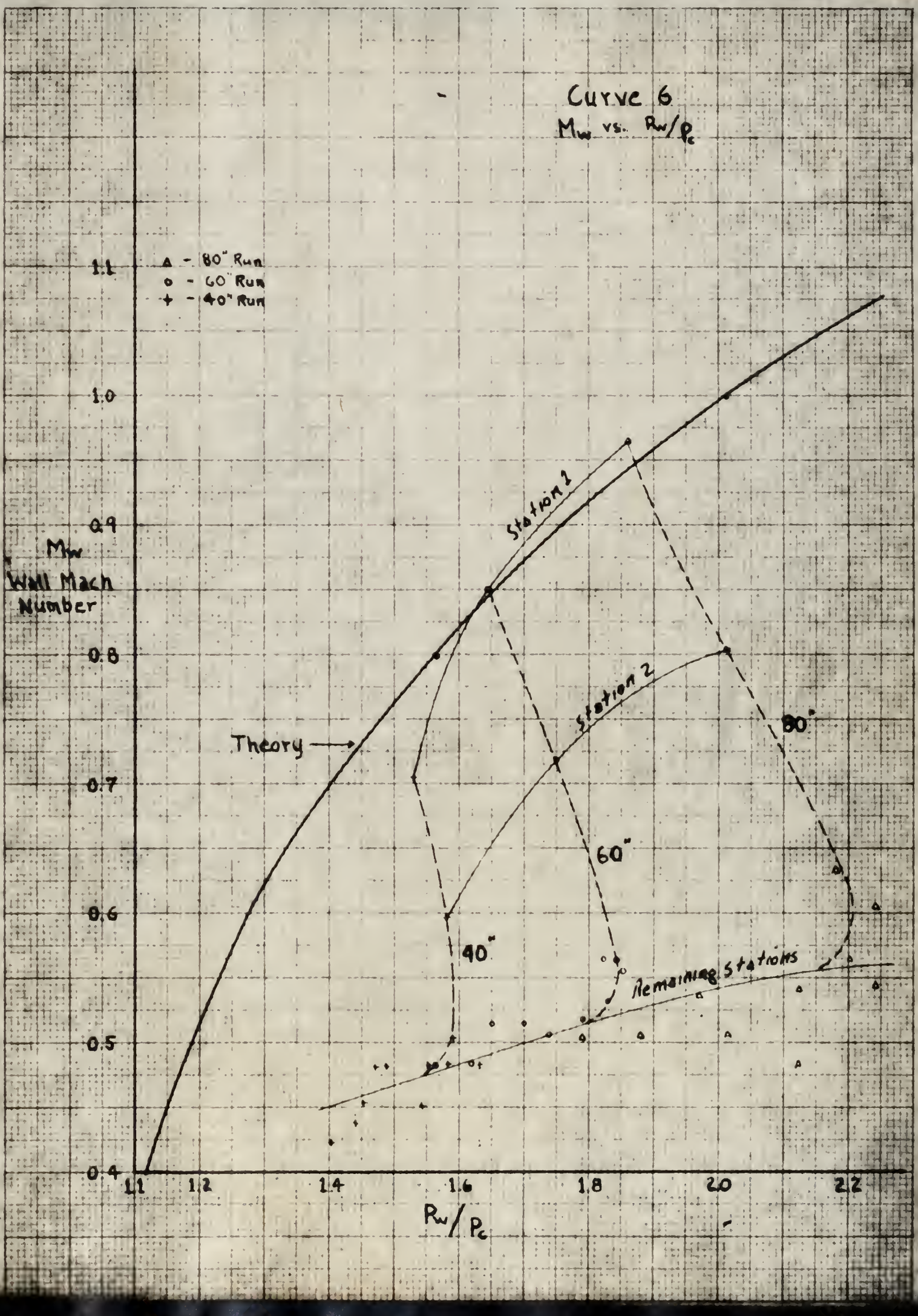
Curve 6
Mw vs. Rw/Pc
Δ - 80" Run
o - 60" Run
+ - 40" Run
Mw
Wall Mach
Number
1.1
1.0
0.9
0.8
0.7
0.6
0.5
0.4
Station 2
Station 2
Theory
80"
60"
40"
Remaining Stations
1.1
1.2
1.4
1.6
1.8
2.0
2.2
Rw/Pc

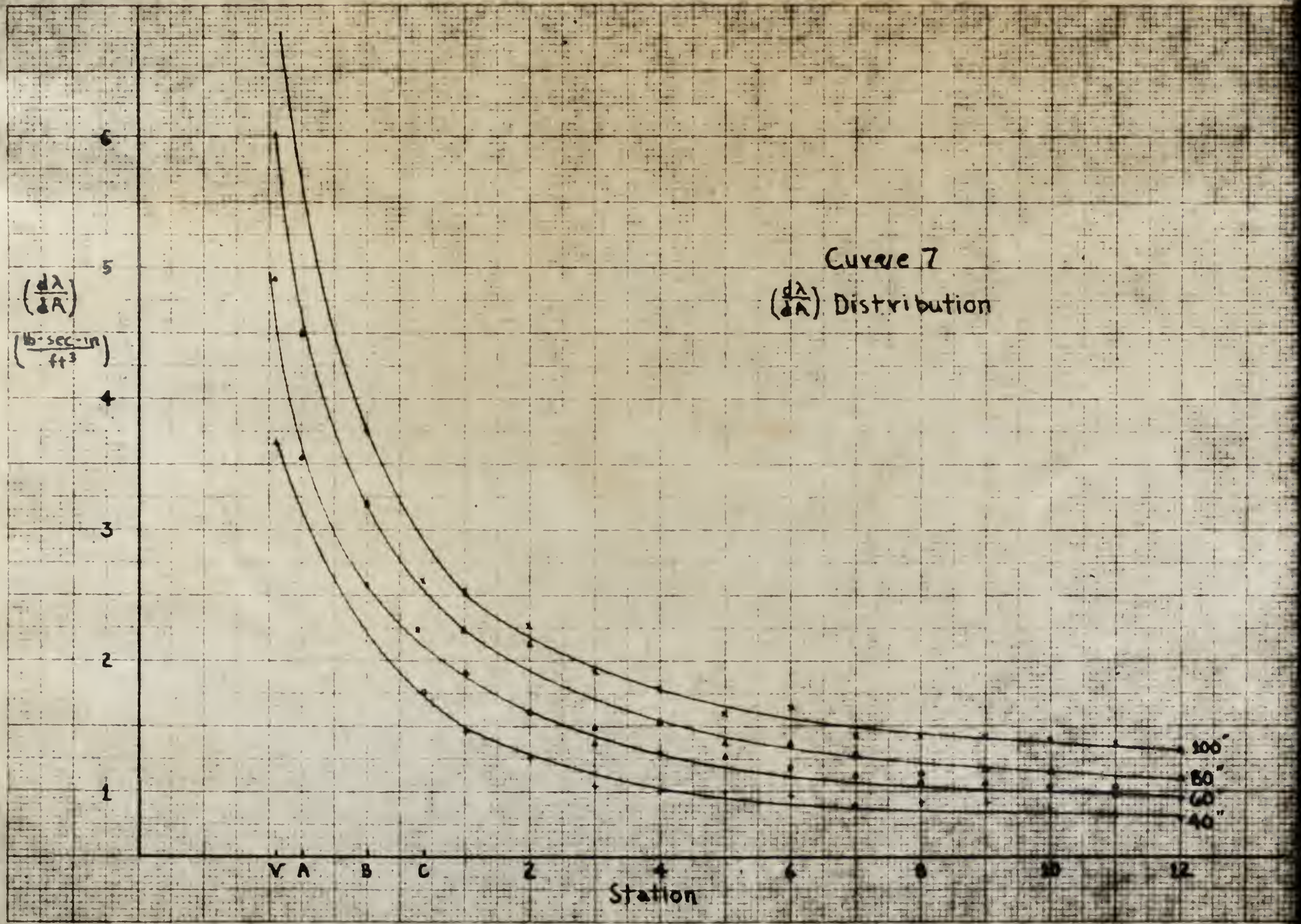
Curve 7
$\left(\frac{d\lambda}{dA}\right)$ Distribution
$\left(\frac{d\lambda}{dA}\right)$
$\left(\frac{lb\text{-}sec^2\text{-}in}{ft^3}\right)$
6
5
4
3
2
1
V
A
B
C
2
4
6
8
10
12
Station
100"
80"
60"
40"

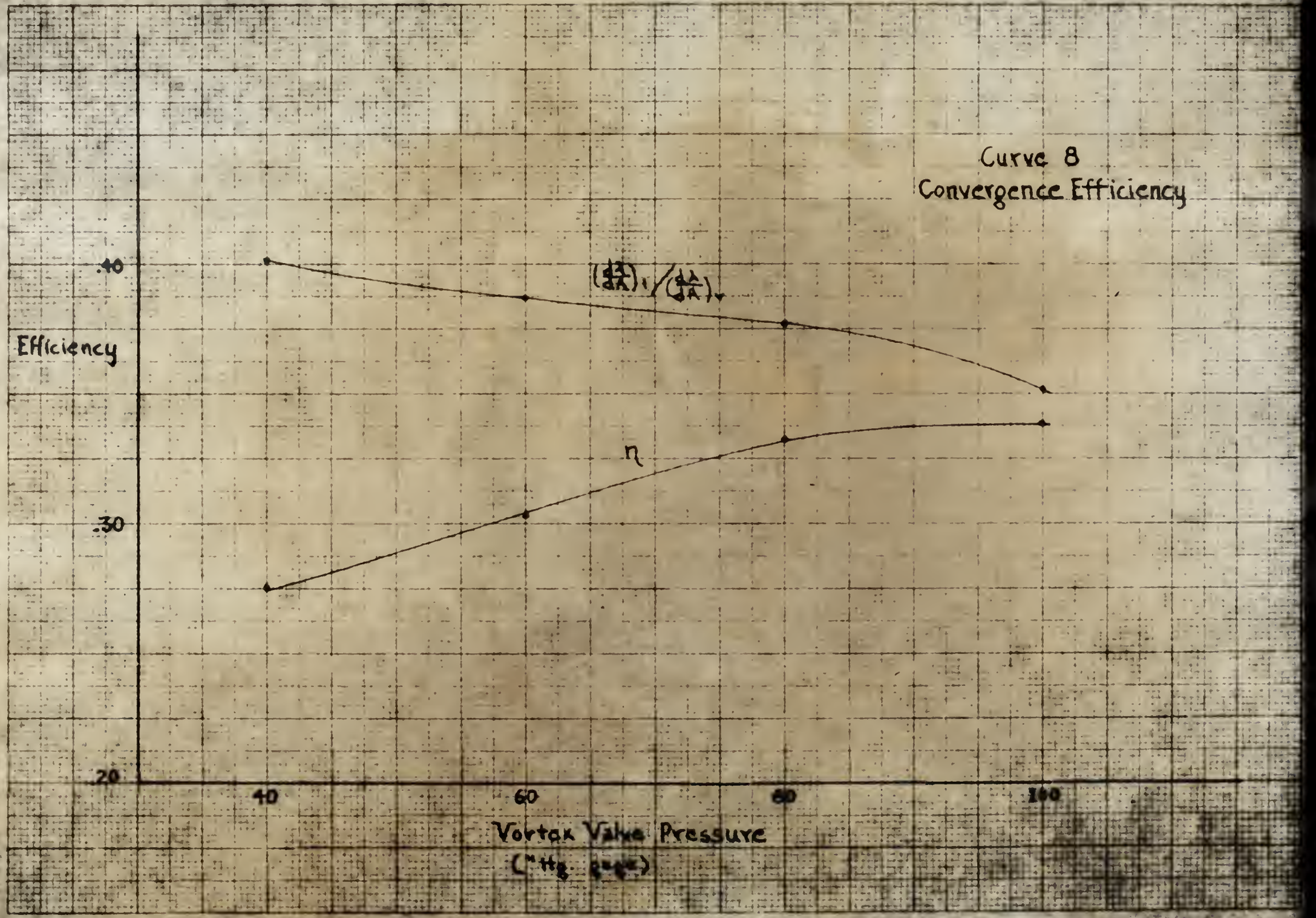
Curve 8
Convergence Efficiency
.40
Efficiency
$(\frac{dP}{dx})_1/(\frac{dP}{dx})_2$
η
.30
.20
40
60
80
100
Vortex Valve Pressure
("Hg. gage)

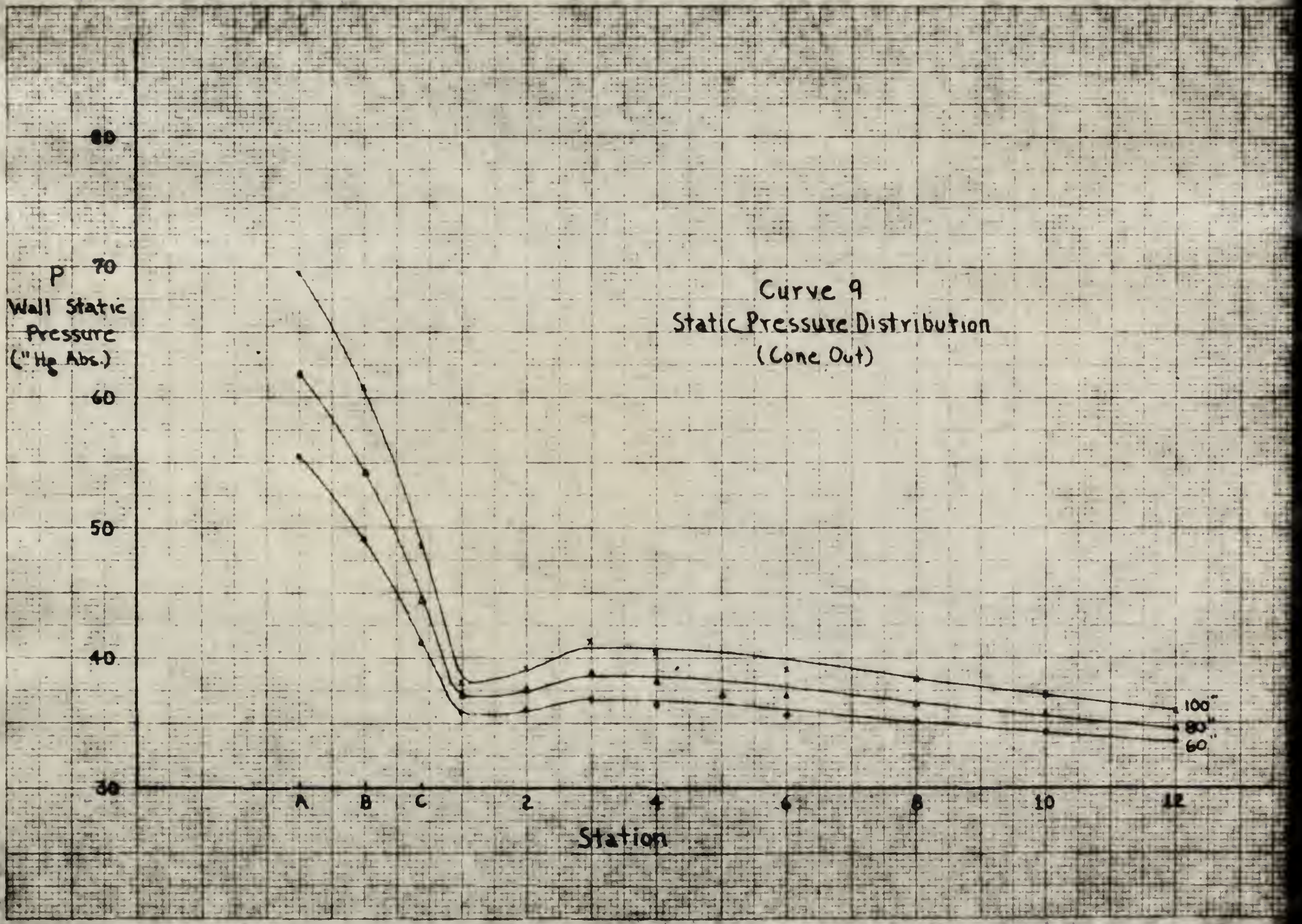
Curve 9
Static Pressure Distribution
(Cone Out)
P
Wall Static Pressure ("Hg Abs.)
80
70
60
50
40
30
A
B
C
2
4
6
8
10
12
Station
100"
80"
60"

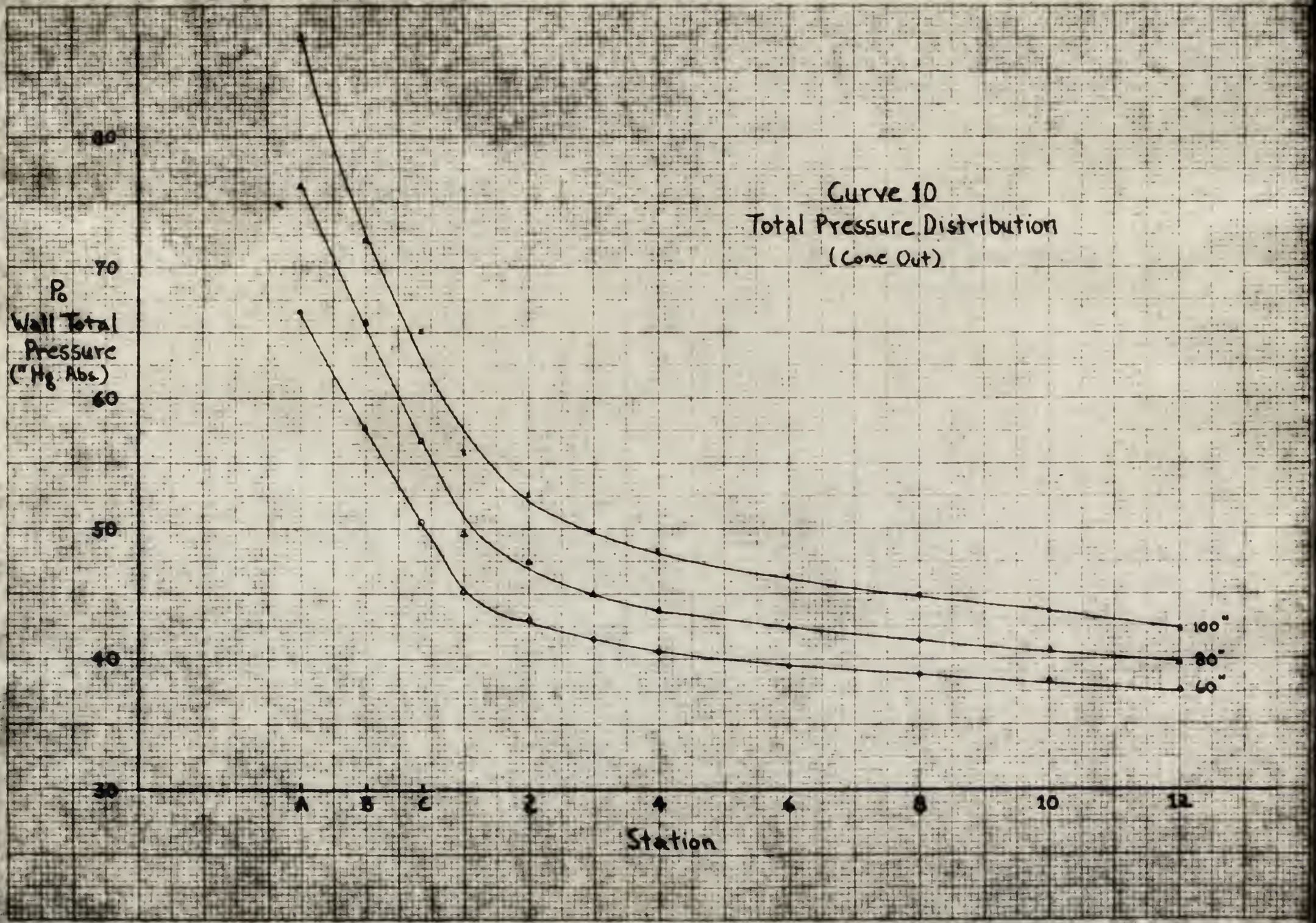
Curve 10
Total Pressure Distribution
(Cone Out)
P_o
Wall Total
Pressure
("Hg Abs.)
80
70
60
50
40
30
A
B
C
2
4
6
8
10
12
Station
100"
80"
60"

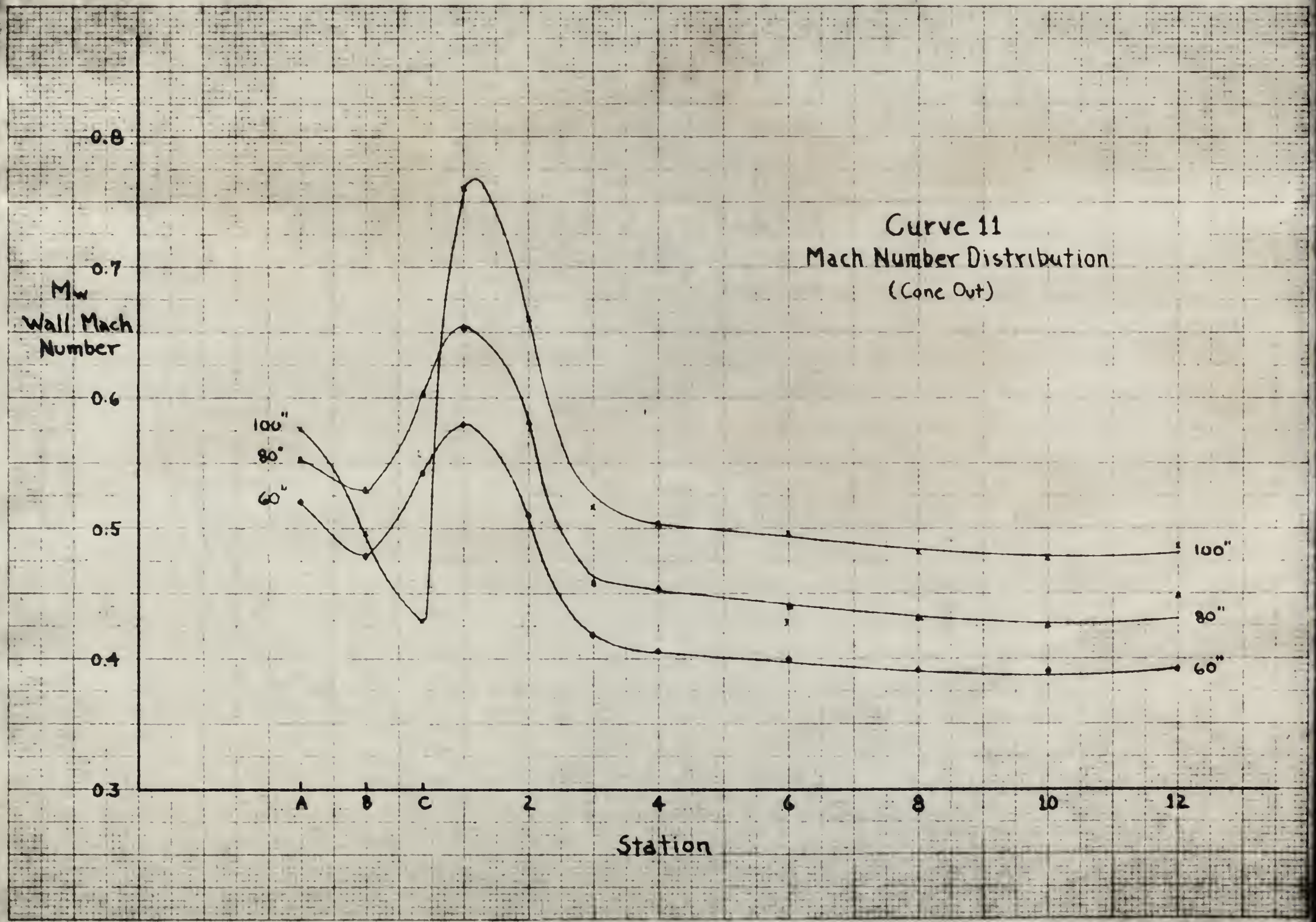
Curve 11
Mach Number Distribution
(Cone Out)
Mw
Wall Mach
Number
0.8
0.7
0.6
0.5
0.4
0.3
100"
80"
60"
A
B
C
2
4
6
8
10
12
Station

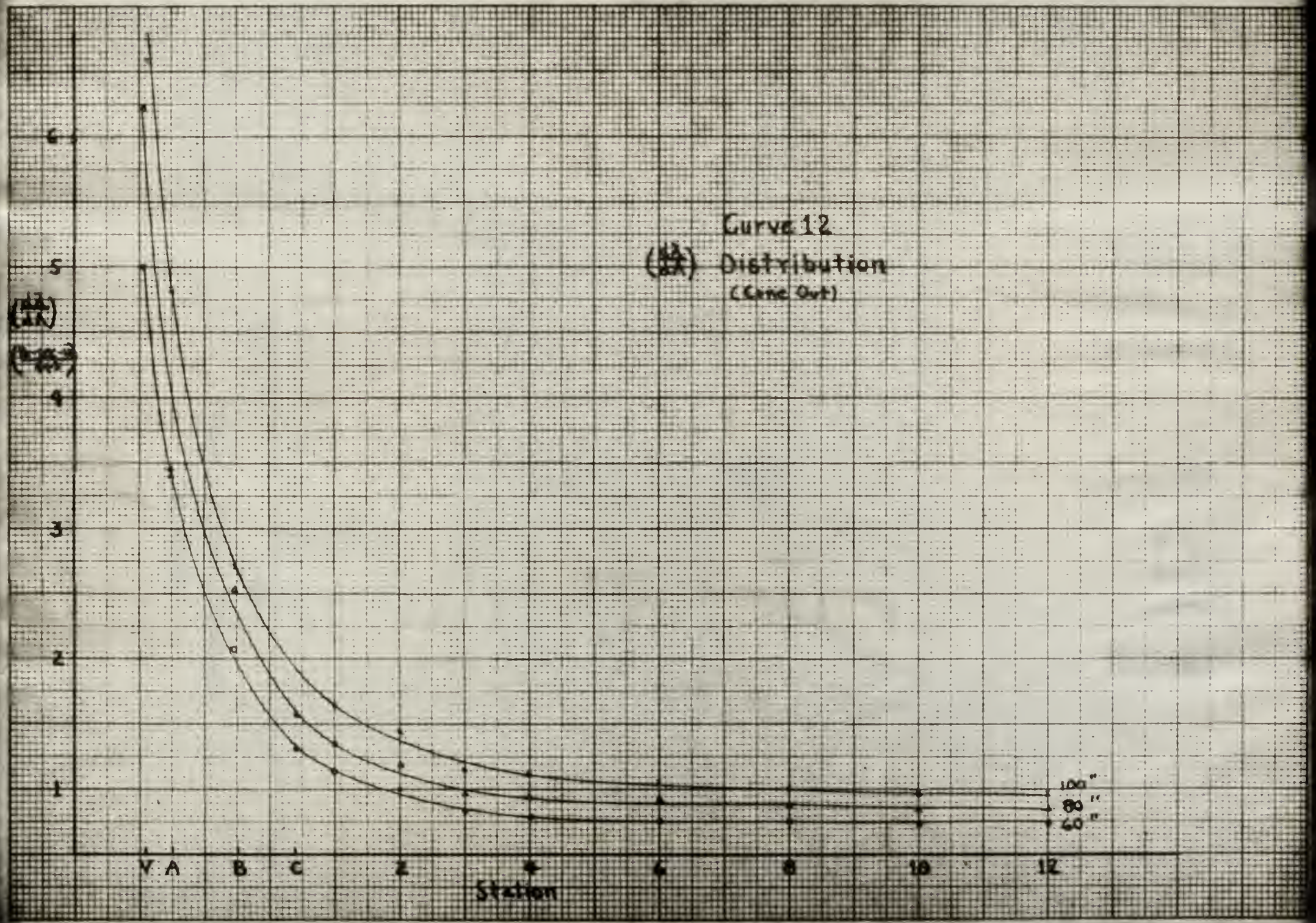
Curve 12
(dh/dx) Distribution
(Cone Out)
6
5
4
3
2
1
100"
80"
60"
V
A
B
C
2
4
6
8
10
12
Station

Curve 13
Convergence Efficiency
(Cone Out)

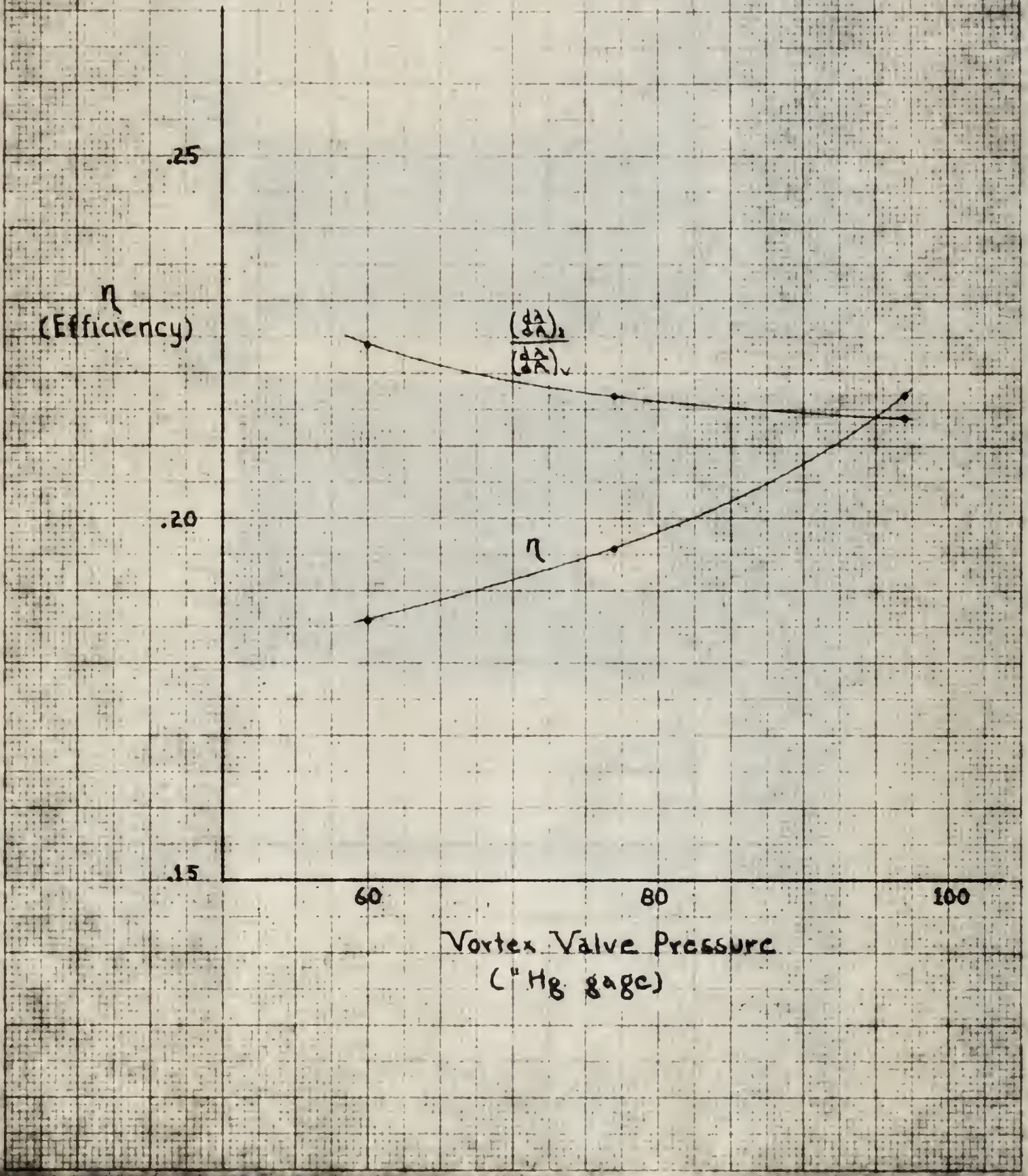

GENERAL VIEW OF EXPERIMENTAL SET-UP

VORTEX TUBE AND NOSE CONE

CONVERGENCE CONE AND VORTEX VALVE

NOSE CONE, AXIAL PROBE, AND "SPIDER" BRACE

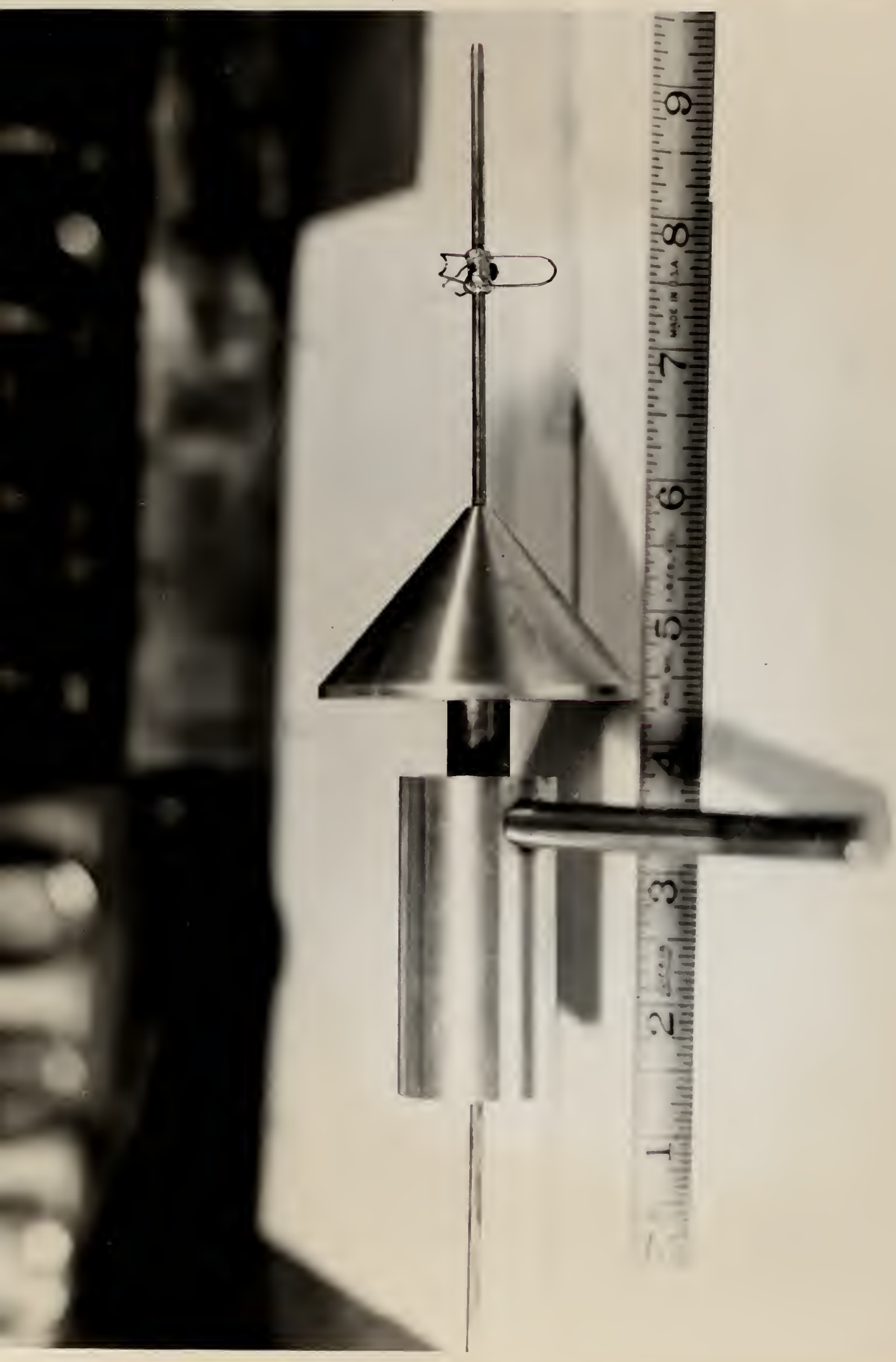

DATE DUE

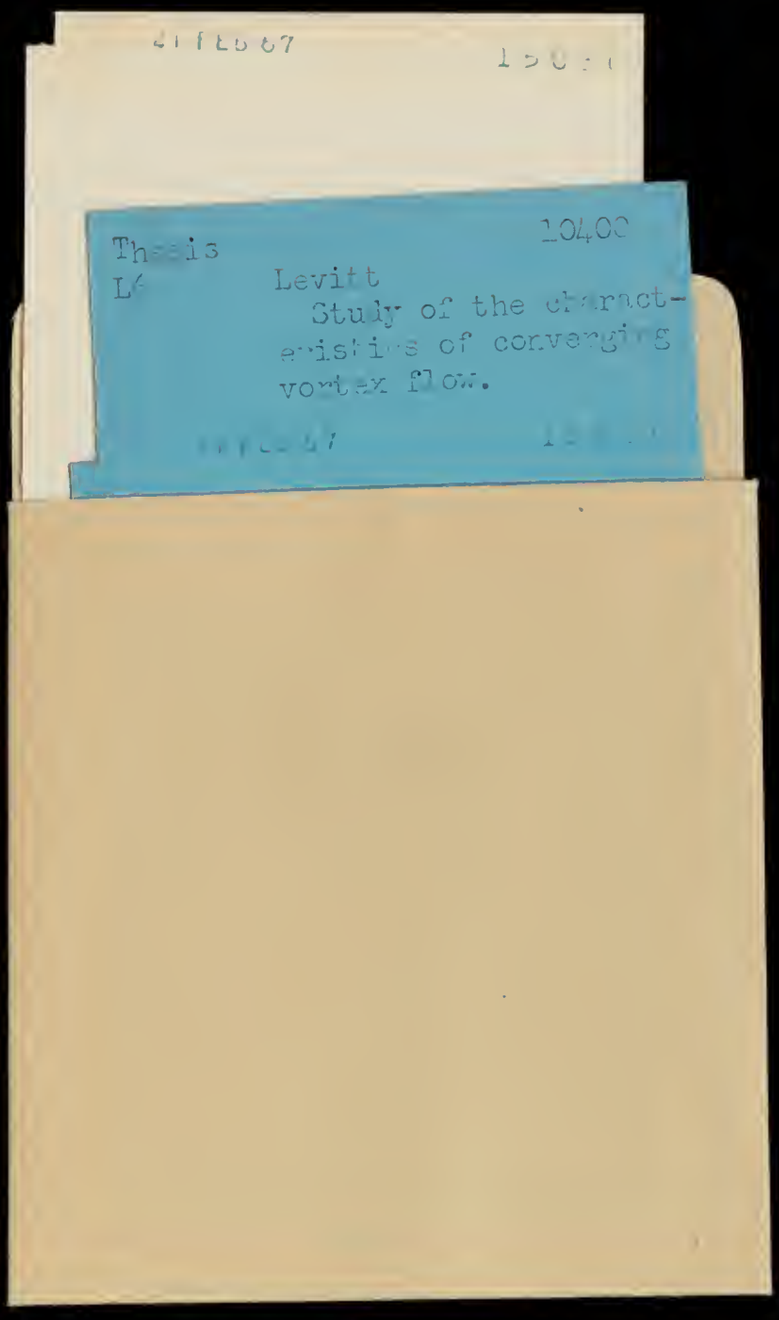

ACCO
FASTENERS FOR BINDING
PRESS BINDER
BGS 2507-EMB
PRODUCTS INCORPORATED

thesL6
A study of the characteristics of conver
3 2768 002 11863 0
DUDLEY KNOX LIBRARY